CONFIDENTIAL

[redacted]

NASA TM X-1705

NASA TECHNICAL MEMORANDUM

AT-TRANSFER MEASUREMENTS
TAINED ON THE X-15 AIRPLANE
CLUDING CORRELATIONS WITH
ND-TUNNEL RESULTS

Robert D. Quinn and Frank V. Olinger

ght Research Center

wards, Calif.

ONAL AERONAUTICS AND SPACE ADMINISTRATION • WASHINGTON, D. C. • MARCH 1969

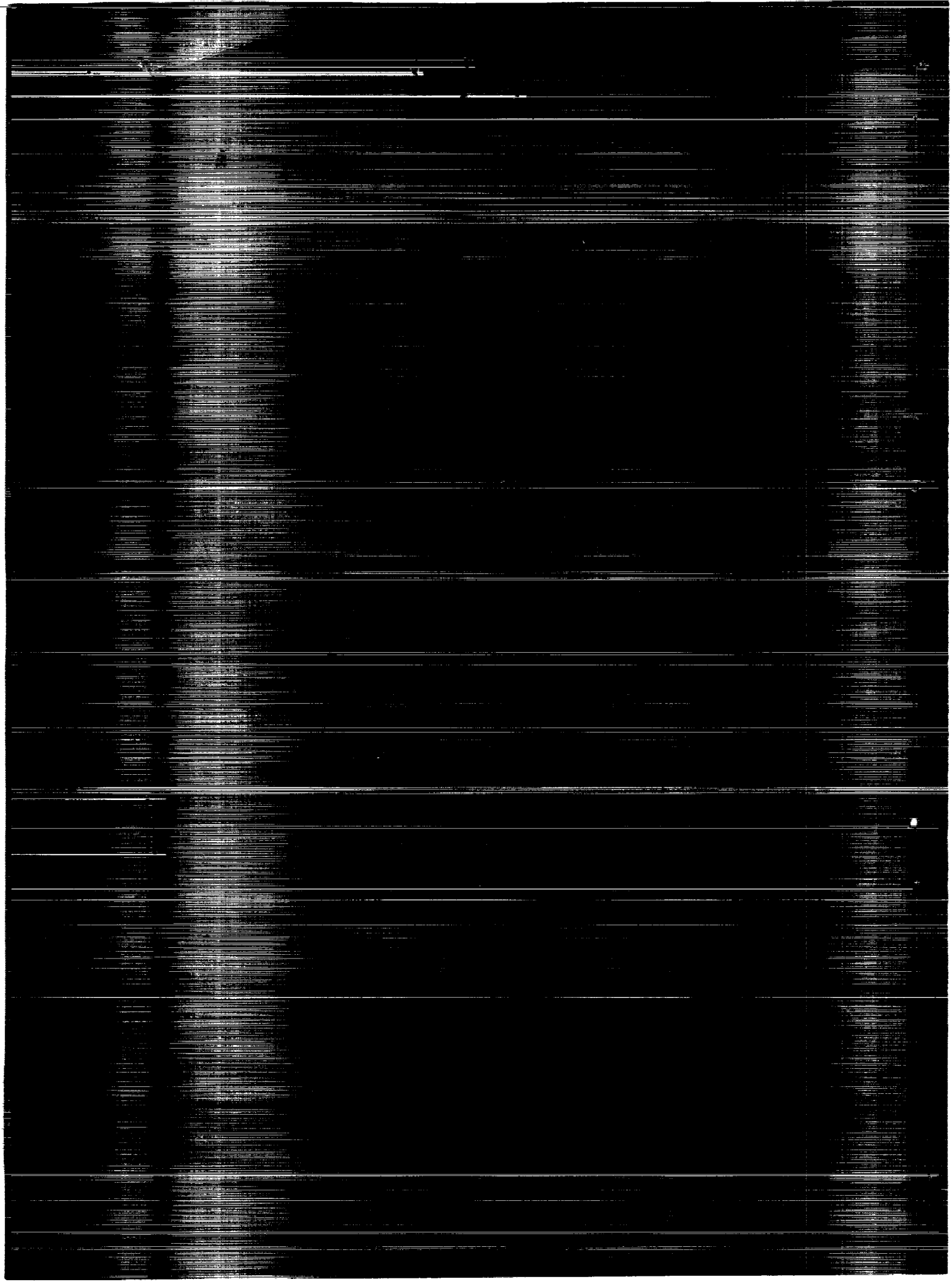

~~CONFIDENTIAL~~

NASA TM X-1705

HEAT-TRANSFER MEASUREMENTS OBTAINED ON THE X-15 AIRPLANE INCLUDING CORRELATIONS WITH WIND-TUNNEL RESULTS

By Robert D. Quinn and Frank V. Olinger

Flight Research Center
Edwards, Calif.

NATIONAL AERONAUTICS AND SPACE ADMINISTRATION

~~CONFIDENTIAL~~

[redacted]

HEAT-TRANSFER MEASUREMENTS OBTAINED ON THE X-15 AIRPLANE INCLUDING CORRELATIONS WITH WIND-TUNNEL RESULTS[1]

By Robert D. Quinn and Frank V. Olinger
Flight Research Center

SUMMARY

Heat-transfer measurements were obtained on the X-15 airplane from two flights under quasi-steady conditions at a free-stream Mach number of 5.1 and an angle of attack of 2.0° and a free-stream Mach number of 4.98 and an angle of attack of 16.3°. These measurements were made at corresponding free-stream Reynolds numbers of 2.45×10^6 and 1.31×10^6 per foot (8.04×10^6 and 4.30×10^6 per meter). Experimental heat-transfer coefficients derived from temperatures obtained from 200 recording thermocouples on the skin of the airplane are tabulated. Correlations with wind-tunnel results show that the wind-tunnel data are in fair-to-good agreement with the flight data obtained on the wing, ventral tail, and vertical tail at low angles of attack but are generally in poor agreement with the high-angle-of-attack data and the low-angle-of-attack fuselage data.

INTRODUCTION

During the X-15 flight program, a substantial amount of temperature, flow field, and heat-transfer data has been obtained at various locations on the airplane. Both skin and structural temperature data are presented in references 1 to 3. References 4 to 8 contain results of flow-field and local-surface static-pressure investigations. References 9 to 13 compare measured and calculated heat-transfer data obtained on the fuselage, wing, and vertical tail. The primary purpose of references 9 to 13 was to determine the adequacy of the various theories to predict turbulent heat transfer; the results of these reports were, therefore, limited to the areas on the airplane where the local flow conditions were known.

The purpose of this report is to present the heat-transfer data obtained on all surfaces of the X-15 airplane and to make correlations with wind-tunnel data where possible. The data presented were obtained from two flights with high heating levels (flights 2-22 and 2-28)[2] during which quasi-steady flight conditions were maintained long enough to enable reliable heat-transfer coefficients to be derived from skin-temperature time histories.

---

[1] Title, Unclassified.

[2] In the flight-designation system used for the X-15 airplane, the first digit is the number of the airplane, and the following digits indicate the flight number.

The accuracy of the wind-tunnel data is discussed in appendix A, prepared by James C. Dunavant and Robert L. Stallings, Jr., of Langley Research Center.

SYMBOLS

The units used for physical quantities in this paper are given both in U.S. Customary Units and the International System of Units (SI). Factors relating the two systems are presented in reference 14; those used in this paper are presented in appendix B.

$\frac{b}{2}$ semispan of wing, 11.18 feet (3.41 meters)

$\frac{b_h}{2}$ semispan of horizontal tail, 9.04 feet (2.76 meters)

b_{ven} span of ventral tail, 6.08 feet (1.85 meters)

b_{ver} span of vertical tail, 6.92 feet (2.11 meters)

$c_{p,w}$ specific heat of skin material, British thermal units per pound (mass)-degrees Rankine (joules per kilogram-degrees Kelvin)

$\bar{c}$ reference chord of wing, 10.65 feet (3.25 meters) (see fig. 3)

$\bar{c}_h$ reference chord of horizontal tail, 4.56 feet (1.39 meters) (see fig. 3)

$\bar{c}_v$ reference chord of vertical and ventral tails, 9.74 feet (2.97 meters) (see fig. 3)

F radiation geometry factor, 1.0

g gravitational conversion factor, 32.17 pounds (mass)-foot per pound-second^2

H enthalpy, British thermal units per pound (mass) (joules per kilogram)

H_R boundary-layer recovery enthalpy, British thermal units per pound (mass) (joules per kilogram)

h geometric altitude, feet (meters)

h_H local heat-transfer coefficient based on enthalpy, pounds (mass) per foot^2-second (kilograms per meter^2-second)

h_T local heat-transfer coefficient based on temperature, British thermal units per foot^2-second-degrees Rankine (joules per meter^2-second-degrees Kelvin)

h_t height of Unitary Plan wind tunnel test section (appendix A)

J	mechanical equivalent of heat, 778 foot-pounds per British thermal unit
l	length of fuselage, 49.5 feet (15.09 meters)
M	Mach number
N_{Pr}	Prandtl number
N_{Re}	Reynolds number, $\frac{\rho V x}{\mu}$
N_{St}	Stanton number (nondimensional heat-transfer coefficient), $\frac{h_H}{\rho V}$
$N_{St,i}$	local incompressible Stanton number (see eq. (6))
p	absolute static pressure, pounds per foot^2 (newtons per meter^2)
q	dynamic pressure, pounds per foot^2 (newtons per meter^2)
T	temperature, degrees Rankine (degrees Kelvin)
T_R	boundary-layer recovery temperature, degrees Rankine (degrees Kelvin)
t	time, seconds
V	velocity, feet per second (meters per second)
x	chordwise distance along wing measured from leading edge, feet (meters)
x_f	axial distance along fuselage measured from nose of fuselage, feet (meters)
x_h	chordwise distance along horizontal tail measured from leading edge, feet (meters)
x_v	chordwise distance along vertical or ventral tail measured from leading edge, feet (meters)
y	distance from vertical plane of symmetry, feet (meters)
z	distance from horizontal plane containing longitudinal axis, feet (meters)
α	airplane angle of attack, degrees
β	angle of sideslip, degrees
$\delta_{h,L}$	left-horizontal-tail deflection, leading edge up positive, degrees
$\delta_{h,R}$	right-horizontal-tail deflection, leading edge up positive, degrees
δ_{SB}	speed-brake deflection, degrees

δ_v vertical- and ventral-tail deflections, leading edge right positive, degrees

ϵ emissivity of skin surface

μ dynamic viscosity, pounds (mass) per foot-second (newton-seconds per meter^2)

η recovery factor

ρ density of air, pounds (mass) per foot^3 (kilograms per meter^3)

ρ_w density of skin material, pounds (mass) per foot^3 (kilograms per meter^3)

σ Stefan-Boltzmann constant, 4.78×10^{-13} British thermal units per foot^2-second-degrees Rankine^4 (5.67×10^{-8} watts per meter^2-degrees Kelvin^4)

τ skin thickness, feet (meters)

φ circumferential angle, zero on lower-fuselage centerline, degrees

Subscripts:

l local

w wall or skin

∞ free stream

Superscript:

* evaluated at reference enthalpy

AIRPLANE AND INSTRUMENTATION

For the type of mission discussed in this report, the X-15 airplane (fig. 1) is launched from a B-52 carrier airplane at about 45,000 feet (13,700 meters) altitude, climbs under full power to the desired altitude, attains level flight at reduced throttle to stabilize the velocity, and, after fuel depletion, performs other required maneuvers and glides to a landing at Edwards Air Force Base, Calif. The data for the experiments discussed in this report were obtained during the periods of quasi-steady flight prior to fuel depletion.

A cutaway drawing of the X-15 fuselage showing the arrangement of the major internal components is presented in figure 2. The anhydrous-ammonia and liquid-oxygen tanks are integral parts of the fuselage structure. The skin of the X-15 airplane is constructed of Inconel X. Physical characteristics of the airplane, fuselage coordinates, and wing and horizontal-tail ordinates are presented in tables I to IV, respectively.

There are 290 thermocouples on the inner surface of the skin on the X-15 airplane. During the two flights used in this analysis, outputs from 200 of these skin thermocouples were recorded. The general location of the 200 thermocouples is shown in

figures 3 and 4(a) and 4(b); table V presents, in detail, the locations of each thermocouple and other pertinent structural information.

The thermocouples are constructed of 30-gage chromel-alumel wires spot-welded to the inner surface of the airplane skin. Outputs from each thermocouple were commutated and recorded at 1-second intervals on an onboard 12-channel NACA oscillograph. The thermocouple measurements were accurate to ±5 R° (±2.78 K°) (ref. 9), and the resolution was ±1 R° (±0.556 K°).

TEST CONDITIONS

Time histories of free-stream velocity, free-stream dynamic pressure, altitude, and angle of attack for flights 2-22 and 2-28 are shown in figures 5(a) and 5(b), respectively. In these figures, the shaded portion of the flight profiles indicates the quasi-steady period during which data were obtained for the heat-transfer analysis. All pertinent flight parameters for this period are listed in table VI. Heat-transfer coefficients were derived at the following conditions:

Flight	M_∞	α, deg	$N_{Re,\infty}$,		p_∞,		T_∞,	
			per foot	per meter	lb/ft^2	hN/m^2	°R	°K
2-22	5.10	2.0	2.45×10^6	8.04×10^6	95	45.5	390	217
2-28	4.98	16.3	1.31	4.30	53	25.4	401	223

DATA REDUCTION

The heat-transfer coefficients were evaluated from the measured temperature time histories by means of the following thin-skin heat-balance equation:

$$\rho_w c_{p,w} \tau \frac{dT_w}{dt} = h_H(H_R - H_w) - \sigma \epsilon F T_w^4 \qquad (1)$$

This equation neglects heat absorbed by the skin from solar radiation and heat lost from internal radiation and conduction. The radiation effects are considered to be negligible for the flight conditions encountered. The heat-transfer data presented in this report have not been corrected for conduction errors. These errors are between 4 percent and 10 percent for the wing midsemispan and upper-vertical-tail midspan and lower-fuselage centerline (refs. 9 and 10). Conduction losses are unknown for the other locations.

By solving equation (1) for the heat-transfer coefficient h_H, the following expression is obtained:

$$h_H = \frac{\rho_w c_{p,w} \tau \frac{dT_w}{dt} + \sigma \epsilon F T_w^4}{H_R - H_w} \qquad (2)$$

where

$$H_W = f(T_W) \quad \text{(ref. 15)}$$

The recovery enthalpy was computed from the relationship

$$H_R = H_\infty + \eta \frac{V_\infty^2}{2gJ} \tag{3}$$

where η is the recovery factor and was taken to be equal to 0.9 for this analysis.

The Stanton numbers tabulated in tables VII and VIII and plotted in figures 6 to 11 were computed by using the equation

$$N_{St,\infty} = \frac{h_H}{\rho_\infty V_\infty} \tag{4}$$

where $\rho_\infty V_\infty$ = 22.54 pounds (mass) per foot^2-second (110.00 kilograms per meter^2-second) and 12.11 pounds (mass) per foot^2-second (59.10 kilograms per meter^2-second) for the test conditions of flights 2-22 and 2-28, respectively.

The heat-transfer coefficients tabulated in tables VII and VIII were obtained from the following relationship:

$$h_T = \frac{h_H(H_R - H_W)}{T_R - T_W} \tag{5}$$

where

$$T_R = f(H_R) \quad \text{(ref. 15)}$$

The skin heating rates $\frac{dT_W}{dt}$ were determined by fitting least-square second-degree curves through 11 data points (10 seconds of data taken during the quasi-steady portion of the flights). The heating rate at the midpoint of each curve was used to compute the heat-transfer coefficient. These heating rates and the wall temperatures for all thermocouple locations are tabulated in tables VII and VIII. The locations of the thermocouples and the skin thicknesses τ were obtained from the X-15 manufacturer's drawings and are presented in table V. The specific heat $c_{p,W}$ was obtained from reference 16. The emissivity ϵ of the test surface had a nominal value of 0.76 (ref. 17). The density ρ_W of Inconel X was a known constant of 515 pounds (mass) per foot^3 (8250 kilograms per meter^3). Values for the heat-storage capacity of the skin $\rho_W c_{p,W} \tau$ are also tabulated in tables VII and VIII.

RESULTS AND DISCUSSION

Measured heat-transfer data in the form of heat-transfer coefficients and Stanton numbers are listed in tables VII and VIII for all locations on the airplane at which skin temperatures were measured. Most of the measured heat-transfer data in tables VII and VIII are also compared to values calculated by the reference enthalpy method (ref. 18). It should be noted that the comparisons with theory were not made to determine the adequacy of the theory but, rather, to compare the level of the measured data to a known level (for example, values predicted by flat-plate theory). The local flow conditions used to obtain the calculated flat-plate heat-transfer coefficients were computed by the tangent-cone method for the fuselage (ref. 9) and by the oblique-shock Prandtl-Meyer expansion theory (with sweep neglected) for the wing and horizontal and vertical tails. Free-stream conditions were assumed to exist ahead of all surfaces.

Effect of Angle of Attack on Heat Transfer

Fuselage. – The nondimensional heat-transfer coefficients (Stanton numbers) measured on the bottom centerline and on or near the top centerline are presented in figures 6(a) and 6(b). Also, flat-plate values predicted by the reference enthalpy method (ref. 18) are shown. As expected, the heat-transfer coefficients measured on the bottom centerline at the high angle of attack (16.3°) are substantially higher than the low-angle-of-attack (2.0°) coefficients. The difference between the data obtained on the upper- and lower-fuselage surfaces is an order of magnitude larger for the high-angle-of-attack flight than for the low-angle-of-attack flight. The effect of angle of attack on the peripheral heat-transfer coefficients is shown in figures 7(a) to 7(g). The calculated Stanton numbers for $\varphi = 0°$ and $\varphi = 180°$ are also presented.

Wing. – Measured Stanton numbers obtained on the lower and upper surfaces of the wing at three span locations are presented in figures 8 and 9. Figure 8 shows the effect of angle of attack on the heat-transfer coefficients measured on the lower surface of the wing. As shown, the high-angle-of-attack data (16.3°) are 3 to 5 times higher than the low-angle-of-attack data (2.0°). Figure 9 shows the effect of angle of attack on the heat-transfer measurements obtained on the upper surface of the wing. As expected, the Stanton numbers obtained at the high angle of attack are lower than the Stanton numbers obtained at the low angle of attack. Also shown in these figures are values predicted by the reference enthalpy method.

Horizontal tail. – Measured heat-transfer coefficients obtained on the upper and lower surfaces of the horizontal tail are presented in figures 10(a) and 10(b). The measured Stanton numbers obtained on the upper surface at the high angle of attack are higher than the corresponding values obtained on the lower surface. Higher heating was expected on the upper surface because the effective angle of attack[1] of the horizontal tail was negative (leading edge down). Also, figure 10 shows that the high-angle-of-attack data measured on both the upper and lower surfaces are considerably higher than

[1]The effective angle of attack of the horizontal tail is equal to the angle of attack α plus the horizontal-tail deflection $\delta_{h,R}$ minus the downwash angle; the downwash angles were -1.3° and 2.4° for flight 2-22 and flight 2-28, respectively (ref. 19).

the low-angle-of-attack data. These higher heating rates probably resulted from the horizontal tail being in a high-pressure region produced by the proximity of the wing shock waves at high angles of attack. The Stanton numbers predicted by the flat-plate theory (ref. 18) for an isolated airfoil are also shown in figure 10. The calculated values do not show the large difference between the upper and lower surfaces at the high angle of attack that is shown by the measured data, which indicates that the downwash angle in flight was larger than the value obtained from reference 19.

Ventral and vertical tails. – Figure 11(a) shows the heat transfer measured on the ventral tail. The data obtained at an angle of attack of 16.3° (flight 2-28) are on the average about 100 percent higher than the data obtained at an angle of attack of 2.0° (flight 2-22). These higher heating rates measured during flight 2-28 resulted from the high pressure in the ventral area produced by the proximity of the bow shock at this high angle of attack (ref. 4). Also shown in figure 11(a), for reference, are the calculated flat-plate values. These calculations do not predict the large differences in heat transfer between flight 2-22 and flight 2-28 that are seen in the measured data because the calculations do not account for the bow-shock effects. The small differences in the calculated heat-transfer coefficients that are shown in figure 11 are due primarily to Reynolds number effect.

Measured Stanton numbers obtained on the vertical tail at the three span locations are shown in figures 11(b), 11(c), and 11(d). As shown, the heat transfer decreases with increasing angle of attack, with the largest decrease occurring at the root station ($\frac{z}{b_{ver}} = 0.455$) and the smallest decrease occurring at the tip station ($\frac{z}{b_{ver}} = 0.963$). These results were expected, since at high angles of attack the vertical tail is in the wake of the fuselage, which results in lower pressures and correspondingly lower heating rates. Stanton numbers computed by the reference enthalpy method are also presented in figures 11(b), 11(c), and 11(d).

Heat-transfer measurements obtained on the speed brake of the ventral and vertical tails are shown in figures 11(a) and 11(b), respectively. The data obtained on the speed brakes show a sharp rise over the data measured forward of the speed brakes. This increase is not a result of speed-brake deflection, since measurements show that the speed brakes were closed (see table VI). It is believed that the increased heating on the speed brakes resulted from a bleedoff of the boundary layer into the low-pressure region behind the hinge-line gap (see fig. 12). This bleedoff would result in a thin boundary layer on the speed brake and, consequently, higher heating rates.

Correlation of Flight and Wind-Tunnel Data

Reynolds number correlations of flight and wind-tunnel data obtained on the lower-fuselage centerline, wing, and ventral and vertical tails for low and high angles of attack are presented in figures 13(a) to 13(f). The wind-tunnel data (ref. 20) were measured at $M_\infty = 4.65$ in the Langley Unitary Plan wind tunnel. The wind-tunnel heat-transfer tests and their accuracy are discussed in appendix A. However, no attempt was made to apply the approximate corrections given in appendix A to the wind-tunnel data presented in the following correlations. To obtain the desired Reynolds number correlation, the measured local Stanton numbers from flight and wind-tunnel tests were transformed to incompressible values by using the reference enthalpy method. The incompressible relationship used in these correlations was based on the Blasius skin-friction law (ref. 21) and Colburn's Reynolds analogy factor (ref. 22), which result in the

following equation:

$$N_{St,i} = \frac{0.0296}{\left(N_{Pr,l}\right)^{2/3}\left(N_{Re,l}\right)^{.2}} \tag{6}$$

Assuming $N_{Pr,l} = 0.726$, equation (6) may be put in the following form:

$$\frac{N_{St,i}}{\left(N_{Re,l}\right)^{.8}} = \frac{0.0366}{\left(N_{Re,l}\right)} \tag{7}$$

By using equation (7) in conjunction with the reference enthalpy method, the following relationship between the compressible local Stanton number and the incompressible local Stanton number can be obtained (ref. 11):

$$\frac{N_{St,l}}{\left(N_{Re,l}\right)^{.8}}\left(\frac{T^*}{T_l}\right)^{.65} = \frac{N_{St,i}}{\left(N_{Re,l}\right)^{.8}} \tag{8}$$

The solid line in figure 13 represents values predicted by equation (7), and the data in these figures are the measured compressible local Stanton numbers that have been reduced to their incompressible values by using equation (8). In this way, the measured data should agree with the solid line in these figures if the reference enthalpy method is assumed to predict correct values of turbulent heat transfer[1]. However, the purpose of figure 13 is not to determine how well the data agree with theory but to show the correlation between flight and wind-tunnel data. The agreement obtained between flight and wind-tunnel data depends to some extent on the theory used to correlate the data, primarily because of the different effect of the ratio of wall-to-recovery temperature on heat transfer predicted by the various theories (refs. 18, 23, and 24) and the fact that the wind-tunnel and flight data were obtained at different temperature ratios. The effect of wall temperature on heat transfer has been the subject of considerable investigation (for example, refs. 24 to 28) but has still not been completely determined. The reference enthalpy method was used to correlate the data in this report because of its wide usage and simplicity, although better agreement would have been obtained if a method that predicts less effect of wall temperature had been chosen (for example, ref. 23). This possibility of improving the correlation between flight and wind-tunnel data by 20 percent to 30 percent was considered when the conclusions were made from the results in figure 13.

Fuselage. – Figure 13(a) shows the flight and wind-tunnel data obtained on the lower-fuselage centerline at high and low angles of attack. The wind-tunnel data are 50 percent to 100 percent higher than the flight data for the low-angle-of-attack condition and about 300 percent higher than the flight data for the high-angle-of-attack condition; the agreement is considered poor. The high heat transfer obtained in the wind tunnel is believed to be the result of roughness effects caused by the transition strip on the model, as discussed in reference 12.

[1]This, of course, also assumes that the local flow conditions used in this analysis are the correct boundary-layer-edge conditions; these local flow conditions were computed in the manner described on page 7.

Wing. – Correlation of flight and wind-tunnel data obtained on the wing at low angles of attack is shown in figure 13(b). The correlation is considered to be good, with the wind-tunnel data averaging 30 percent higher than the flight data. Figure 13(c) shows the correlation of the high-angle-of-attack data. For this condition the agreement between flight and wind-tunnel data is poor, with the wind-tunnel data being generally 100 percent higher than the flight data.

Ventral and vertical tails. – Correlation of flight and wind-tunnel data obtained on the ventral and vertical tails at low angles of attack is presented in figure 13(d). The agreement between flight and wind-tunnel data is considered to be fair, even though the wind-tunnel data are 50 percent to 60 percent higher than the flight data. Figure 13(e) shows the correlation of data obtained on the ventral tail at high angles of attack. The wind-tunnel data are 300 percent higher than the flight data, and the correlation is considered poor. Figure 13(f) shows the correlation between flight and wind-tunnel data obtained on the vertical tail at high angles of attack. Only the data obtained at the midspan station ($\frac{z}{b_{ver}}$ = 0.670 and 0.729 for wind tunnel and flight, respectively) and the tip station ($\frac{z}{b_{ver}}$ = 0.890 and 0.963 for wind tunnel and flight, respectively) are presented. The agreement between the flight and wind-tunnel data at the midspan station is good, but the data obtained at the tip station are only in fair agreement, with the wind-tunnel data being approximately 60 percent higher than the flight data.

CONCLUDING REMARKS

Heat-transfer coefficients were obtained at 200 locations on the X-15 airplane at a free-stream Mach number of 5.1 and an angle of attack of 2.0° and a free-stream Mach number of 4.98 and an angle of attack of 16.3°. The data obtained showed the effect of angle of attack on the distribution of heat-transfer coefficients on the fuselage, wing, horizontal tail, and ventral and vertical tails. As expected, an increase in the angle of attack resulted in (1) increased differences between the data obtained on the upper and lower fuselage and wing surfaces, (2) increased ventral-tail heating, and (3) decreased vertical-tail heating. In addition, increasing angle of attack resulted in higher heating on the upper and lower surfaces of the horizontal tail.

Correlations of the measured data obtained on the fuselage, wing, and ventral and vertical tails with wind-tunnel results showed that the high-angle-of-attack wind-tunnel data were generally in poor agreement with the flight data. Also, the correlation of the low-angle-of-attack fuselage data was poor. However, good agreement was obtained between the low-angle-of-attack flight and wind-tunnel data measured on the lower surface of the wing, and correlation was fair between the flight and wind-tunnel data measured on the ventral and vertical tails at low angles of attack.

Flight Research Center,
National Aeronautics and Space Administration,
Edwards, Calif., July 31, 1968,
719-01-00-03-24.

APPENDIX A

HEAT-TRANSFER MEASUREMENTS ON THE X-15 IN THE LANGLEY UNITARY PLAN WIND TUNNEL AT MACH 4.65

By James C. Dunavant and Robert L. Stallings, Jr.
Langley Research Center

The purpose of this appendix is to discuss the wind-tunnel tests reported in reference 20 and errors in the heat-transfer measurements which resulted from a transient nonuniform vertical temperature distribution found in the tunnel subsequent to the tests.

The X-15 heat-transfer coefficients were determined from the transient skin temperature response to an increase in the tunnel total temperature. The increase is obtained during operation by quickly bypassing the cooler between the last compressor and the test section. Before the temperature increase, the model is at recovery temperature and the ratio measured at that time of recovery temperature to total temperature is assumed to be constant through the transient. The heat-transfer coefficient is evaluated from an integral form of the calorimeter equation (eq. (4) of ref. 20) using the transient difference between the recovery temperature (calculated from the constant ratio of recovery temperature to total temperature) and model skin temperature.

Total-temperature surveys along the vertical centerline at Mach 4.65 in the Unitary Plan wind tunnel during a transient total-temperature increase are shown in figure 14. The increase is usually between 54 R° (30 K°) and 81 R° (45 K°), and the heat-transfer data-taking period is 15 seconds, starting about 6 seconds after opening of the bypass ($t = 0$ in fig. 14). The highest temperatures were measured near the top of the tunnel, and, although not shown in the figure, the temperatures in a horizontal plane through the tunnel centerline were approximately uniform.

The 0.0667-scale X-15 model was mounted below the center of the tunnel by using an offset sting, as shown in figure 15, to allow for movement to 28° angle of attack. In these tests, total temperature was measured at thermocouples (also shown in fig. 15) attached to the strut at a point aft of the ventral tail but displaced to one side about 9.72 in. (12 cm) from the tunnel vertical centerline. The two shielded probes were mounted so that one was approximately alined to the flow at low angle of attack and the other at high angle of attack. At $\alpha = 0°$ the stagnation thermocouples were located about 4.72 in. (12 cm) below the centerline of the model. Rotating the model to 15° angle of attack placed the forward instrumented section ($\frac{x_f}{l}$ = 0 to 34.3) about 3.15 in. (8 cm) to 5.91 in. (15 cm) above the tunnel centerline, while the stagnation thermocouples were about 9.84 in. (25 cm) below. The total-temperature difference between the two vertical stations from figure 14 is from 12.6 R° (7 K°) to 25.2 R° (14 K°), which would produce an estimated error in heat-transfer coefficient of 50 percent. For locations on the model nearer the stagnation-temperature-measurement location, the error would be less. However, where heating (and, hence, wall temperature) is high, thereby reducing the difference ($T_R - T_w$), greater errors in the heat-transfer

coefficients result. Exact determination of the error can be made only from temperature histories of the model and the tunnel stagnation temperature at the appropriate vertical station. The zero angle-of-attack results would have a minimum error because the model and stagnation thermocouple "see" approximately the same stream.

The large vertical transient temperature did not exist at the other test Mach number of 2.88 in reference 20. At this Mach number, the increase in heating with angle of attack over the bottom forward fuselage was consistent with theory but deviated greatly at Mach 4.65. Thus, only the high angle-of-attack results at Mach 4.65 appear to be incorrect.

APPENDIX B

CONVERSION OF U. S. CUSTOMARY UNITS TO SI UNITS

The International System of Units (SI) was adopted by the Eleventh General Conference on Weights and Measures, Paris, October 1960, in Resolution No. 12 (ref. 14). Conversion factors for the units used herein are given in the following table:

Physical quantity	U. S. Customary Unit	Conversion factor*	SI Unit
Density	lbm/ft^3	16.02	kg/m^3
Enthalpy	Btu/lbm	2.32×10^3	J/kg
Specific heat	Btu/lbm-°R	4.18×10^3	J/kg-°K
Heat-transfer coefficient	Btu/ft^2-sec-°R	2.042×10^4	J/m^2-sec-°K
Length	ft	0.3048	m
	in.	2.54	cm
Pressure	lb/ft^2	0.4788	hN/m^2
Temperature	°R	0.556	°K
Dynamic viscosity	lbm/ft-sec	1.488	$N\text{-sec}/m^2$
Velocity	ft/sec	0.3048	m/sec

*Multiply value given in U. S. Customary Unit by conversion factor to obtain equivalent value in SI Unit.

Prefixes to indicate multiple of units are:

Prefix	Multiple
centi (c)	10^{-2}
hecto (h)	10^2
kilo (k)	10^3

REFERENCES

1. Gord, P. R.: Measured and Calculated Structural Temperature Data From Two X-15 Airplane Flights With Extreme Aerodynamic Heating Conditions. NASA TM X-1358, 1967.

2. Watts, Joe D.; and Banas, Ronald P.: X-15 Structural Temperature Measurements and Calculations for Flights to Maximum Mach Numbers of Approximately 4, 5, and 6. NASA TM X-883, 1963.

3. Reed, Robert D.; and Watts, Joe D.: Skin and Structural Temperatures Measured on the X-15 Airplane During a Flight to a Mach Number of 3.3. NASA TM X-468, 1961.

4. McLain, L. J.; and Palitz, Murray: Flow-Field Investigations on the X-15 Airplane and Model Up to Hypersonic Speeds. NASA TN D-4813, 1968.

5. Palitz, Murray: Measured and Calculated Flow Conditions on the Forward Fuselage of the X-15 Airplane and Model at Mach Numbers From 3.0 to 8.0. NASA TN D-3447, 1966.

6. Pyle, Jon S.: Flight Pressure Distributions on the Vertical Stabilizers and Speed Brakes of the X-15 Airplane at Mach Numbers From 1 to 6. NASA TN D-3048, 1965.

7. Pyle, Jon S.: Flight-Measured Wing Surface Pressures and Loads for the X-15 Airplane at Mach Numbers From 1.2 to 6.0. NASA TN D-2602, 1965.

8. Pyle, Jon S.: Comparison of Flight Pressure Measurements With Wind-Tunnel Data and Theory for the Forward Fuselage of the X-15 Airplane at Mach Numbers From 0.8 to 6.0. NASA TN D-2241, 1964.

9. Quinn, Robert D.; and Palitz, Murray: Comparison of Measured and Calculated Turbulent Heat Transfer on the X-15 Airplane at Angles of Attack Up to 19.0°. NASA TM X-1291, 1966.

10. Banas, Ronald P.: Comparison of Measured and Calculated Turbulent Heat Transfer in a Uniform and Nonuniform Flow Field on the X-15 Upper Vertical Fin at Mach Numbers of 4.2 and 5.3. NASA TM X-1136, 1965.

11. Quinn, Robert D.; and Kuhl, Albert E.: Comparison of Flight-Measured and Calculated Turbulent Heat Transfer on the X-15 Airplane at Mach Numbers From 2.5 to 6.0 at Low Angles of Attack. NASA TM X-939, 1964.

12. Banner, Richard D.; Kuhl, Albert E.; and Quinn, Robert D.: Preliminary Results of Aerodynamic Heating Studies on the X-15 Airplane. NASA TM X-638, 1962.

13. Banner, Richard D.; and Kuhl, Albert E.: A Summary of X-15 Heat-Transfer and Skin-Friction Measurements. NASA TM X-1210, 1966.

14. Mechtly, E. A.: The International System of Units - Physical Constants and Conversion Factors. NASA SP-7012, 1964.

15. Hansen, C. Frederick: Approximations for the Thermodynamic and Transport Properties of High-Temperature Air. NASA TR R-50, 1959. (Supersedes NACA TN 4150.)

16. Sachs, G.; and Pray, R. Ford, III, eds.: Air Weapons Materials Application Handbook Metals and Alloys, First ed., TR 59-66, USAF Air Res. and Develop. Command, Dec. 1959. (Available from ASTIA as AD 252301.)

17. Ohlsen, P. E.; and Etemad, G. A.: Spectral and Total Radiation Data of Various Aircraft Materials. Rep. No. NA 57-330, North American Aviation, Inc. (Los Angeles, Calif.), July 23, 1957.

18. Eckert, Ernst R. G.: Survey of Boundary Layer Heat Transfer at High Velocities and High Temperatures. WADC Tech. Rep. 59-624, Wright Air Dev. Center, U. S. Air Force, Apr. 1960. (Available from ASTIA as AD 238292.)

19. Binz, E. F.: Basic Aerodynamic Characteristics X-15 Research Airplane. Rep. No. NA-58-299, North American Aviation, Inc. (Los Angeles, Calif.), Feb. 12, 1958.

20. Price, Earl A.; Taylor, Nancy L.; and Burbank, Paige B.: Heat-Transfer Measurements of a 0.0667-Scale Model of the X-15 Airplane for an Angle-of-Attack Range of 0° to 28° at Mach Numbers of 2.88 and 4.65. NASA TM X-821, 1963.

21. Eckert, E. R. G.; and Drake, Robert M., Jr.: Heat and Mass Transfer. Second ed., McGraw-Hill Book Co., Inc., 1959, p. 270.

22. Colburn, Allan P.: A Method of Correlating Forced Convection Heat Transfer Data and a Comparison With Fluid Friction. Trans. Amer. Inst. Chem. Eng., vol. 29, 1933, pp. 174-210.

23. Spalding, D. B.; and Chi, S. W.: The Drag of a Compressible Turbulent Boundary Layer on a Smooth Flat Plate With and Without Heat Transfer. J. Fluid Mech., vol. 18, part I, Jan. 1964, pp. 117-143.

24. Winkler, Eva M.; and Cha, Moon H.: Investigation of Flat Plate Hypersonic Turbulent Boundary Layers With Heat Transfer at a Mach Number of 5.2. NAVORD Rep. 6631 (Aerodynamics Res. Rep. No. 60), U. S. Naval Ordnance Lab., White Oak, Md., Sept. 15, 1959.

25. Sommer, Simon C.; and Short, Barbara J.: Free-Flight Measurements of Turbulent-Boundary-Layer Skin Friction in the Presence of Severe Aerodynamic Heating at Mach Numbers From 2.8 to 7.0. NACA TN 3391, 1955.

26. Tendeland, Thorval: Effects of Mach Number and Wall-Temperature Ratio on Turbulent Heat Transfer at Mach Numbers From 3 to 5. NASA TR R-16, 1959. (Supersedes NACA TN 4236.)

27. Bertram, Mitchel H.; Cary, Aubrey M., Jr.; and Whitehead, Allen H., Jr.: Experiments With Hypersonic Turbulent Boundary Layers on Flat Plates and Delta Wings. NASA paper presented at AGARD Specialists' Meeting on Hypersonic Boundary Layers and Flow Fields (London, England), May 1-3, 1968.

28. Samuels, Richard D.; Peterson, John B., Jr.; and Adcock, Jerry B.: Experimental Investigation of the Turbulent Boundary Layer at a Mach Number of 6 With Heat Transfer at High Reynolds Numbers. NASA TN D-3858, 1967.

TABLE I. – PHYSICAL CHARACTERISTICS OF THE X-15 AIRPLANE

Wing –	
Airfoil section	NACA 66005 (modified)
Total area (includes 94.98 ft^2 (8.82 m^2) covered by fuselage), ft^2 (m^2)	200 (18.58)
Span, ft (m)	22.36 (6.82)
Mean aerodynamic chord, ft (m)	10.27 (3.13)
Root chord, ft (m)	14.91 (4.54)
Tip chord, ft (m)	2.98 (0.91)
Taper ratio	0.20
Aspect ratio	2.50
Sweep at leading edge, deg	36.75
Sweep at 25-percent-chord line, deg	25.64
Sweep at trailing edge, deg	-17.74
Incidence, deg	0
Horizontal tail –	
Airfoil section	NACA 66005 (modified)
Total area (includes 63.29 ft^2 (5.88 m^2) covered by fuselage), ft^2 (m^2)	115.34 (10.72)
Span, ft (m)	18.08 (5.51)
Mean aerodynamic chord, ft (m)	7.05 (2.15)
Root chord, ft (m)	10.22 (3.12)
Tip chord, ft (m)	2.11 (0.64)
Taper ratio	0.21
Aspect ratio	2.83
Sweep at leading edge, deg	50.58
Sweep at 25-percent-chord line, deg	45
Sweep at trailing edge, deg	19.28
Ratio horizontal-tail area to wing area	0.58
Upper vertical tail–	
Airfoil section	10° single wedge
Area (excluding area covered by fuselage), ft^2 (m^2)	40.91 (3.80)
Span, ft (m)	6.92 (2.11)
Mean aerodynamic chord, ft (m)	8.95 (2.73)
Root chord, ft (m)	10.21 (3.11)
Tip chord, ft (m)	7.56 (2.30)
Taper ratio	0.74
Aspect ratio	0.51
Sweep at leading edge, deg	30
Sweep at 25-percent-chord line, deg	23.41
Ratio vertical-tail area to wing area	0.20
Speed-brake total surface area, ft^2 (m^2)	11.18 (1.04)
Lower vertical tail –	
Airfoil section	10° single wedge
Area (excluding area covered by fuselage), ft^2 (m^2)	34.41 (3.20)
Span, ft (m)	6.17 (1.88)
Mean aerodynamic chord, ft (m)	9.17 (2.80)
Root chord, ft (m)	10.21 (3.11)
Tip chord, ft (m)	8.00 (2.44)
Taper ratio	0.78
Aspect ratio	0.43
Sweep at leading edge, deg	30
Sweep at 25-percent-chord line, deg	23.41
Ratio vertical-tail area to wing area	0.17
Speed-brake total surface area, ft^2 (m^2)	11.18 (1.04)
Fuselage –	
Length, ft (m)	49.5 (15.09)
Maximum width, ft (m)	7.33 (2.23)
Maximum depth, ft (m)	4.67 (1.42)
Maximum depth over canopy, ft (m)	4.97 (1.51)
Side area (total), ft^2 (m^2)	215.66 (20.03)
Fineness ratio	10.91
Sweep at canopy leading edge, deg	60

TABLE II. – FUSELAGE CONTOUR COORDINATES

$\frac{x_f}{l}$, percent (a)	Fuselage station	Radius,	
		in.	cm
0.54	1.6	3.270	8.31
.77	3.0	3.656	9.29
1.11	5.0	4.195	10.66
1.95	10.0	5.513	14.00
2.79	15.0	6.792	17.25
3.64	20.0	8.032	20.40
4.48	25.0	9.233	23.45
5.32	30.0	10.396	26.41
6.16	35.0	11.520	29.26
7.00	40.0	12.605	32.02
7.84	45.0	13.652	34.68
8.68	50.0	14.662	37.24
10.37	60.0	16.566	42.08
12.05	70.0	18.322	46.54
13.73	80.0	19.928	50.62
15.42	90.0	21.386	54.32
17.10	100.0	22.697	57.65
20.47	120.0	24.882	63.20
23.83	140.0	26.487	67.28
28.88	170.0	27.817	70.66
31.75	187.0	28.000	71.12
90.00	533.0	28.000	71.12
95.38	565.0	26.548	67.43
99.25	588.0	24.000	60.96

[a] l = 594 in. (1509 cm). Fuselage station 0 located at $\frac{x_f}{l}$ = 0.27 percent.

TABLE III. – WING AIRFOIL ORDINATES[a]

[NACA 66005 modified[b]]

Percent chord	$\frac{y}{b/2}$ = 0.357 (wing station 47.88[c])				$\frac{y}{b/2}$ = 0.629 (wing station 84.50[c])				$\frac{y}{b/2}$ = 0.953 (wing station 127.67[c])			
	Distance to leading edge,		Ordinate,		Distance to leading edge,		Ordinate,		Distance to leading edge,		Ordinate,	
	in.	cm	in.	cm	in.	cm	in.	cm	in.	cm	in.	cm
0	0	0	0	0	0	0	0	0	0	0	0	0
Tangent point	.38	.97	.37	.94	.38	.97	.37	.94	.38	.97	.37	.94
.88	1.12	2.84	.42	1.07	.78	1.98	.40	1.02	.38	.97	.37	.94
1.25	1.60	4.06	.55	1.40	1.11	2.82	.47	1.19	.54	1.37	.40	1.02
5.00	6.39	16.23	1.15	2.92	4.44	11.28	.87	2.21	2.16	5.49	.51	1.30
10.00	12.78	32.46	1.79	4.55	8.88	22.56	1.27	3.23	4.32	10.97	.64	1.63
15.00	19.17	48.69	2.26	5.74	13.32	33.83	1.66	4.22	6.48	16.46	.75	1.91
20.00	25.56	64.92	2.56	6.50	17.76	45.11	1.79	4.55	8.64	21.95	.86	2.18
25.00	31.95	81.15	2.79	7.09	22.20	56.39	1.96	4.98	10.80	27.43	.93	2.36
32.00	40.90	103.89	3.02	7.67	28.42	72.19	2.12	5.38	13.82	35.10	1.01	2.57
38.00	48.56	123.34	3.14	7.98	33.74	85.70	2.20	5.59	16.42	41.71	1.05	2.67
44.00	56.23	142.82	3.20	8.13	39.07	99.24	2.24	5.69	19.01	48.29	1.07	2.72
50.00	63.90	162.31	3.18	8.08	44.40	112.78	2.23	5.66	21.60	54.86	1.05	2.67
55.90	71.44	181.46	3.10	7.87	49.64	126.09	2.17	5.51	24.15	61.34	1.04	2.64
61.90	79.11	200.94	2.94	7.47	54.97	139.62	2.15	5.46	26.74	67.92	.98	2.49
68.00	86.90	220.73	2.61	6.63	60.38	153.37	1.83	4.65	29.38	74.63	.73	1.85
75.00	95.85	243.46	2.18	5.54	66.60	169.16	1.52	3.86	32.40	82.30	.73	1.85
100.00	127.80	324.61	.66	1.68	88.80	225.55	.45	1.14	43.20	109.73	.21	.53

[a]Measured from chord line.

[b]Leading-edge radius 0.375 in. (0.953 cm) constant, tangent to leading-edge. Basic airfoil modified forward of 17-percent plane and modified to straight side aft of 67-percent plane to 1-percent blunt trailing edge.

[c]Wing side-fairing juncture at wing station 44.00 ($\frac{y}{b/2}$ = 0.328).

TABLE IV. – HORIZONTAL-TAIL AIRFOIL ORDINATES[a]

[NACA 66005 modified[b]]

Percent chord	$\frac{y}{b_h/2}$ = 0.434 (butt plane 47.00)				$\frac{y}{b_h/2}$ = 0.696 (butt plane 75.50)				$\frac{y}{b_h/2}$ = 0.966 (butt plane 104.75)			
	Distance to leading edge,		Ordinate,		Distance to leading edge,		Ordinate,		Distance to leading edge,		Ordinate,	
	in.	cm	in.	cm	in.	cm	in.	cm	in.	cm	in.	cm
0	0	0	0	0	0	0	0	0	0	0	0	0
.10	.81	2.06	.21	.53	.55	1.40	.13	.33	.29	.74	.10	.25
1.25	1.01	2.57	.53	1.35	.69	1.75	.33	.84	.36	.91	.26	.66
5.00	4.02	10.21	.84	2.13	2.74	6.96	.43	1.09	1.43	3.63	.34	.86
10.00	8.05	20.45	1.18	3.00	5.49	13.94	.61	1.55	2.86	7.26	.43	1.09
25.00	20.11	51.08	1.75	4.45	13.72	34.85	.90	2.29	7.16	18.19	.62	1.57
45.00	36.20	91.95	2.01	5.11	24.69	62.71	1.03	2.62	12.88	32.72	.71	1.80
60.00	48.27	122.61	1.89	4.80	32.92	83.62	.97	2.46	17.17	43.61	.67	1.70
67.00	53.90	136.91	1.63	4.14	36.76	93.37	.86	2.18	19.18	48.72	.58	1.47
[c]100.00	80.45	204.34	.40	1.02	54.87	139.37	.27	.69	28.62	72.69	.14	.36

[a]Airfoil ordinates measured perpendicular to chord plane.

[b]Leading-edge radius at root and tip thermocouple stations, 0.500 in. (1.27 cm) and 0.250 in. (0.64 cm), respectively, normal to the leading edge. Root modified forward of 5-percent chord. Tip modified forward of 15-percent chord. Horizontal-tail side-fairing juncture at butt plane 42.74 ($\frac{y}{b_h/2}$ = 0.396).

[c]Airfoil tapers linearly from 67-percent to 100-percent chord.

TABLE V. – THERMOCOUPLE LOCATIONS AND WALL THICKNESSES

(a) Fuselage[a]

Thermocouple	$\frac{x_f}{l}$	φ, deg	τ, ft	τ, m
1	0.047	0	0.0113	0.00345
2	.047	36	.0102	.00310
3	.047	64	.0075	.00229
4	.047	100	.0066	.00201
5	.047	128	.0066	.00201
6	.047	169	.0066	.00201
7	.047	260	.0066	.00201
8	.080	166	.0058	.00178
9	.080	265	.0058	.00178
10	.125	0	.0063	.00191
11	.125	60	.0059	.00180
12	.125	130	.0048	.00147
13	.125	154	.0048	.00147
14	.125	260	.0048	.00147
15	.137	166	.0042	.00127
16	.137	180	.0104	.00318
17	.150	0	.0045	.00137
18	.150	45	.0045	.00137
19	.150	85	.0045	.00137
20	.150	135	.0042	.00127
21	.150	180	.0104	.00318
22	.150	275	.0045	.00137
23	.169	180	.0104	.00318
24	.200	2	.0043	.00132
25	.200	43	.0043	.00132
26	.200	135	.0042	.00127
27	.200	167	.0042	.00127
28	.200	180	.0042	.00127
29	.200	270	.0043	.00132
30	.309	0	.0043	.00132
31	.309	45	.0043	.00132
32	.309	135	.0043	.00132
33	.309	180	.0042	.00127
34	.326	170	.0053	.00160
35	.343	33	.0043	.00132
36	.343	44	.0043	.00132
37	.343	60	.0043	.00132
38	.343	80	.0031	.00094
39	.343	90	.0031	.00094
40	.343	124	.0108	.00328
41	.343	138	.0053	.00160
42	.343	152	.0053	.00160
43	.567	80	.0027	.00081
44	.567	86	.0027	.00081
45	.567	94	.0027	.00081
46	.567	100	.0027	.00081
47	.567	107	.0027	.00081
48	.567	124	.0053	.00160
49	.567	150	.0053	.00160
50	.567	180	.0053	.00160

[a]See figure 4.

(b) Wing upper surface

Thermocouple	$\frac{x}{c}$	$\frac{y}{b/2}$	τ, ft	τ, m
51	0.028	0.357	0.0058	0.00175
52	.056	.357	.0058	.00175
53	.104	.357	.0057	.00173
54	.132	.357	.0056	.00170
55	.181	.357	.0055	.00168
56	.278	.357	.0073	.00224
57	.341	.357	.0073	.00224
58	.403	.357	.0073	.00224
59	.459	.357	.0073	.00224
60	.639	.357	.0073	.00224
61	.674	.357	.0073	.00224
62	.744	.357	.0073	.00224
63	.834	.357	.0032	.00097
64	.890	.357	.0032	.00097
65	.938	.357	.0032	.00097
66	.028	.629	.0048	.00145
67	.049	.629	.0048	.00145
68	.070	.629	.0048	.00145
69	.132	.629	.0048	.00145
70	.188	.629	.0057	.00173
71	.229	.629	.0057	.00173
72	.278	.629	.0057	.00173
73	.320	.629	.0057	.00173
74	.382	.629	.0057	.00173
75	.424	.629	.0057	.00173
76	.473	.629	.0057	.00173
77	.521	.629	.0057	.00173
78	.612	.629	.0032	.00097
79	.653	.629	.0032	.00097
80	.688	.629	.0055	.00168
81	.021	.953	.0035	.00107
82	.035	.953	.0035	.00107
83	.049	.953	.0035	.00107
84	.097	.953	.0037	.00112
85	.118	.953	.0037	.00112
86	.139	.953	.0037	.00112
87	.160	.953	.0037	.00112
88	.195	.953	.0037	.00112
89	.222	.953	.0037	.00112
90	.243	.953	.0037	.00112
91	.278	.953	.0033	.00102
92	.313	.953	.0033	.00102

TABLE V. – THERMOCOUPLE LOCATIONS AND WALL THICKNESSES - Continued

(c) Wing lower surface

Thermocouple	$\frac{x}{c}$	$\frac{y}{b/2}$	τ,	
			ft	m
93	0.028	0.357	0.0062	0.00188
94	.056	.357	.0062	.00188
95	.104	.357	.0062	.00188
96	.132	.357	.0062	.00188
97	.181	.357	.0062	.00188
98	.209	.357	.0062	.00188
99	.278	.357	.0053	.00163
100	.341	.357	.0053	.00163
101	.403	.357	.0053	.00163
102	.459	.357	.0053	.00163
103	.619	.357	.0053	.00163
104	.674	.357	.0053	.00163
105	.744	.357	.0053	.00163
106	.834	.357	.0032	.00097
107	.938	.357	.0032	.00097
108	.028	.629	.0049	.00150
109	.049	.629	.0049	.00150
110	.070	.629	.0049	.00150
111	.132	.629	.0049	.00150
112	.188	.629	.0045	.00137
113	.229	.629	.0045	.00137
114	.278	.629	.0045	.00137
115	.320	.629	.0045	.00137
116	.382	.629	.0045	.00137
117	.424	.629	.0045	.00137
118	.473	.629	.0045	.00137
119	.521	.629	.0045	.00137
120	.612	.629	.0032	.00097
121	.653	.629	.0032	.00097
122	.021	.953	.0036	.00109
123	.063	.953	.0036	.00109
124	.097	.953	.0035	.00107
125	.118	.953	.0035	.00107
126	.139	.953	.0035	.00107
127	.160	.953	.0035	.00107
128	.181	.953	.0035	.00107
129	.202	.953	.0035	.00107
130	.222	.953	.0035	.00107
131	.243	.953	.0035	.00107
132	.278	.953	.0033	.00102
133	.313	.953	.0033	.00102
134	.334	.953	.0033	.00102

(d) Horizontal-tail upper surface

Thermocouple	$\frac{x_h}{\bar{c}_h}$	$\frac{y}{b_h/2}$	τ,	
			ft	m
135	0.189	0.696	0.0042	0.00127
136	.281	.696	.0042	.00127
137	.410	.696	.0042	.00127
138	.531	.696	.0042	.00127
139	.640	.696	.0042	.00127
140	.741	.696	.0042	.00127
141	.899	.696	.0042	.00127

(e) Horizontal-tail lower surface

Thermocouple	$\frac{x_h}{\bar{c}_h}$	$\frac{y}{b_h/2}$	τ,	
			ft	m
142	0.189	0.696	0.0042	0.00127
143	.281	.696	.0042	.00127
144	.410	.696	.0042	.00127
145	.531	.696	.0042	.00127
146	.640	.696	.0042	.00127
147	.899	.696	.0042	.00127

TABLE V. – THERMOCOUPLE LOCATIONS AND WALL THICKNESSES - Concluded

(f) Vertical tail

Thermocouple	$\frac{x_v}{\bar{c}_v}$	$\frac{z}{b_{ver}}$	τ,	
			ft	m
148	0.037	0.455	0.0078	0.00236
149	.060	.455	.0059	.00180
150	.120	.455	.0031	.00094
151	.150	.455	.0031	.00094
152	.251	.455	.0017	.00051
153	.300	.455	.0017	.00051
154	.380	.455	.0017	.00051
155	.509	.455	.0017	.00051
156	.560	.455	.0017	.00051
157	.611	.455	.0017	.00051
158	.690	.455	.0109	.00333
159	.709	.455	.0106	.00323
160	.770	.455	.0095	.00290
161	.840	.455	.0088	.00269
162	.910	.455	.0079	.00241
163	.970	.455	.0072	.00218
164	.030	.729	.0082	.00249
[a]164L	.030	.729	.0082	.00249
165	.050	.729	.0065	.00198
165L	.050	.729	.0065	.00198
166	.132	.729	.0031	.00094
166L	.132	.729	.0031	.00094
167	.160	.729	.0031	.00094
167L	.160	.729	.0031	.00094
168	.220	.729	.0031	.00094
168L	.220	.729	.0031	.00094
169L	.261	.729	.0031	.00094
170	.370	.729	.0025	.00076
170L	.370	.729	.0025	.00076
171	.520	.729	.0025	.00076
171L	.520	.729	.0025	.00076
172	.660	.729	.0025	.00076
172L	.660	.729	.0025	.00076
173	.730	.729	.0025	.00076
174	.801	.729	.0025	.00076
174L	.801	.729	.0025	.00076
175	.050	.963	.0071	.00216
176	.160	.963	.0031	.00094
177	.251	.963	.0031	.00094
178	.431	.963	.0025	.00076
179	.580	.963	.0025	.00076
180	.690	.963	.0025	.00076

[a]L indicates thermocouple on left side.

(g) Ventral tail

Thermocouple	$\frac{x_v}{\bar{c}_v}$	$\frac{z}{b_{ven}}$	τ,	
			ft	m
181	0.037	0.517	0.0078	0.00236
182	.060	.517	.0059	.00180
183	.120	.517	.0031	.00094
184	.251	.517	.0031	.00094
185	.300	.517	.0017	.00051
186	.380	.517	.0017	.00051
187	.509	.517	.0017	.00051
188	.560	.517	.0017	.00051
189	.611	.517	.0017	.00051
190	.690	.517	.0109	.00333
191	.709	.517	.0106	.00323

TABLE VI. – FLIGHT PARAMETERS

t, sec	M_∞	p_∞,		T_∞,		α, deg	β, deg	$\delta_{h,L}$, deg	$\delta_{h,R}$, deg	δ_V, deg	δ_{SB}, deg
		lb/ft^2	hN/m^2	°R	°K						
Flight 2-22											
76	4.95	97	46.4	390	217	1.6	0.07	-5.4	-4.3	-0.39	0
77	4.99	96	46.0	390	217	1.6	.07	-5.1	-4.1	-.46	0
78	5.02	96	46.0	390	217	1.8	.11	-4.5	-3.7	-.50	0
79	5.06	95	45.5	390	217	1.7	.03	-4.0	-3.6	-.50	0
80	5.08	95	45.5	390	217	1.9	.07	-3.4	-3.7	-.50	0
[a]81	5.10	95	45.5	390	217	2.0	.04	-3.9	-3.8	-.24	0
82	5.12	95	45.5	390	217	2.0	.19	-4.1	-4.1	-.28	0
83	5.14	95	45.5	390	217	1.9	.19	-4.4	-4.3	-.31	0
84	5.16	95	45.5	390	217	2.2	.19	-4.5	-4.5	-.28	0
85	5.19	95	45.5	390	217	2.2	.21	-4.7	-4.4	-.28	0
86	5.21	95	45.5	390	217	2.2	.21	-4.6	-4.7	-.28	0
Flight 2-28											
83	4.82	57	27.3	400	222	15.7	-.76	-16.2	-15.8	-.03	0
84	4.85	56	26.8	400	222	16.1	-.06	-15.8	-16.0	-1.18	0
85	4.88	55	26.3	400	222	16.3	.82	-16.4	-15.4	.47	0
86	4.91	55	26.3	401	223	16.6	-.72	-16.3	-15.3	-.65	0
87	4.94	54	25.9	401	223	16.0	.58	-15.8	-15.4	-.46	0
[a]88	4.98	53	25.4	401	223	16.3	-.74	-15.5	-15.0	-.11	0
89	5.00	53	25.4	401	223	15.9	.08	-15.3	-14.3	-1.14	0
90	5.03	52	24.9	401	223	15.2	-.36	-14.3	-14.3	-.09	0
91	5.06	52	24.9	402	223	16.3	-.42	-14.5	-14.1	-1.14	0
92	5.09	51	24.4	402	223	16.0	.68	-15.4	-14.6	.21	0
93	5.12	51	24.4	402	223	16.7	-.68	-15.3	-15.1	-.56	0

[a]Time at which heat-transfer coefficients were derived.

TABLE VII. – HEAT-TRANSFER MEASUREMENTS ON FLIGHT 2-22

(a) Fuselage

Thermocouple	$\frac{T_w}{T_R}$	T_w,		$\frac{dT_w}{dt}$,		$\rho_w c_{p,w} \tau$,		h_T,		$N_{St,\infty}$
		°R	°K	R° per sec	K° per sec	$\frac{Btu}{ft^2-°R}$	$\frac{J}{m^2-°K}$	$\frac{Btu}{ft^2-sec-°R}$	$\frac{J}{m^2-sec-°K}$	
1	0.429	896	498	14.5	8.06	0.675	13,780	0.00839	171.3	0.00140
2	.437	913	508	16.0	8.90	.609	12,440	.00848	173.3	.00142
3	.433	906	504	15.7	8.73	.447	9,130	.00612	124.9	.00102
4	.492	1029	572	17.5	9.73	.405	8,270	.00703	143.6	.00117
5	.487	1019	567	18.2	10.12	.405	8,270	.00722	192.0	.00120
6	.497	1040	578	17.0	9.45	.408	8,330	.00697	185.4	.00116
7	.521	1090	606	18.7	10.40	.411	8,390	.00816	166.8	.00136
8	.494	1033	574	15.9	8.84	.293	5,980	.00477	97.5	.00080
9	.523	1095	609	17.5	9.73	.366	7,470	.00691	141.1	.00115
10	.467	977	543	17.5	9.73	.378	7,720	.00623	127.1	.00104
11	.478	1000	556	17.5	9.73	.359	7,330	.00608	124.2	.00101
12	.490	1026	570	17.6	9.79	.293	5,980	.00519	106.0	.00087
13	.491	1028	572	16.0	8.90	.293	5,980	.00478	97.6	.00080
14	.527	1104	614	17.0	9.45	.300	6,130	.00569	116.1	.00095
15	.446	932	518	14.9	8.28	.251	5,130	.00345	70.4	.00058
16	-----	----	---	----	-----	-----	------	-------	-----	-------
17	.506	1059	589	17.4	9.67	.277	5,660	.00509	103.9	.00085
18	.515	1077	599	18.4	10.23	.280	5,720	.00554	113.1	.00092
19	.510	1066	593	16.6	9.23	.277	5,660	.00492	100.4	.00082
20	-----	----	---	----	-----	-----	------	-------	-----	-------
21	-----	----	---	----	-----	-----	------	-------	-----	-------
22	.506	1059	589	16.5	9.17	.277	5,660	.00485	99.1	.00081
23	-----	----	---	----	-----	-----	------	-------	-----	-------
24	.507	1061	590	16.8	9.34	.266	5,430	.00478	97.5	.00080
25	.492	1029	572	16.7	9.29	.265	5,411	.00454	92.7	.00076
26	-----	----	---	----	-----	-----	------	-------	-----	-------
27	-----	----	---	----	-----	-----	------	-------	-----	-------
28	-----	----	---	----	-----	-----	------	-------	-----	-------
29	.488	1020	567	14.8	8.23	.264	5,390	.00399	81.5	.00067
30	.412	861	479	9.9	5.50	.256	5,230	.00221	45.2	.00037
31	.408	854	475	10.8	6.00	.256	5,230	.00238	48.7	.00040
32	-----	----	---	----	-----	-----	------	-------	-----	-------
33	-----	----	---	----	-----	-----	------	-------	-----	-------
34	.423	884	492	10.0	5.56	.363	7,410	.00320	65.3	.00054
35	.402	840	467	11.9	6.62	.254	5,190	.00256	52.4	.00043
36	.394	823	458	11.2	6.23	.254	5,190	.00238	48.5	.00040
37	.413	864	480	10.4	5.78	.256	5,230	.00234	47.7	.00039
38	.522	1093	608	16.6	9.23	.192	3,920	.00370	75.5	.00062
39	.488	1021	568	15.6	8.67	.189	3,860	.00311	63.5	.00052
40	.283	591	329	4.7	2.61	.587	11,990	.00186	37.9	.00032
41	.321	670	373	11.7	6.51	.298	6,090	.00250	51.0	.00042
42	.374	782	435	11.0	6.12	.306	6,250	.00267	54.5	.00045
43	.453	947	527	12.8	7.12	.160	3,270	.00204	41.7	.00034
44	.582	1219	678	20.5	11.40	.171	3,490	.00490	100.0	.00081
45	.462	966	537	13.8	7.67	.162	3,310	.00225	46.0	.00038
46	.383	801	445	9.5	5.28	.155	3,170	.00125	25.6	.00021
47	.414	866	481	10.7	5.95	.158	3,230	.00155	31.6	.00026
48	.334	699	389	6.4	3.56	.300	6,130	.00144	29.4	.00024
49	.354	739	411	7.0	3.89	.302	6,170	.00166	33.8	.00028
50	.411	860	478	11.6	6.45	.310	6,330	.00308	63.0	.00052

TABLE VII. – HEAT-TRANSFER MEASUREMENTS ON FLIGHT 2-22 - Continued

(b) Wing upper surface

Thermocouple	$\frac{T_w}{T_R}$	T_w,		$\frac{dT_w}{dt}$,		$\rho_w c_{p,w} \tau$,		h_T,		$N_{St,\infty}$
		°R	°K	R° per sec	K° per sec	$\frac{Btu}{ft^2\text{-}°R}$	$\frac{J}{m^2\text{-}°K}$	$\frac{Btu}{ft^2\text{-}sec\text{-}°R}$	$\frac{J}{m^2\text{-}sec\text{-}°K}$	
51	0.401	838	466	10.2	5.67	0.338	6,900	0.00288	58.9	0.00048
52	.423	884	492	9.8	5.45	.343	7,000	.00298	60.8	.00050
53	.464	970	539	17.4	9.67	.345	7,050	.00563	114.9	.00094
54	.442	925	514	15.3	8.51	.332	6,780	.00457	93.3	.00076
55	.424	886	493	14.2	7.90	.328	6,700	.00406	82.8	.00068
56	.343	716	398	8.3	4.61	.419	8,560	.00260	53.0	.00044
57	.345	721	401	7.6	4.23	.419	8,560	.00243	49.6	.00041
58	.340	710	395	7.3	4.06	.419	8,560	.00227	46.3	.00038
59	.338	707	393	6.9	3.84	.418	8,540	.00216	44.1	.00037
60	.313	653	363	5.1	2.84	.415	8,470	.00151	30.8	.00026
61	.300	627	349	4.3	2.39	.407	8,310	.00123	25.2	.00021
62	.303	634	353	4.2	2.34	.407	8,310	.00121	24.8	.00021
63	.373	779	433	6.5	3.61	.185	3,780	.00102	20.9	.00017
64	.377	788	438	7.3	4.06	.185	3,780	.00115	23.4	.00019
65	.377	788	438	7.2	4.00	.185	3,780	.00113	23.0	.00019
66	.777	1327	738	26.4	14.68	.311	6,350	.01166	238.0	.00193
67	.593	1242	691	22.8	12.68	.304	6,210	.00921	188.1	.00153
68	.536	1121	623	20.6	11.45	.297	6,070	.00673	137.4	.00112
69	.519	1085	603	20.1	11.18	.294	6,000	.00624	127.4	.00104
70	.431	901	501	15.5	8.62	.336	6,860	.00457	93.3	.00076
71	.422	883	491	14.3	7.95	.336	6,860	.00415	84.8	.00070
72	.410	858	477	13.4	7.45	.333	6,800	.00378	77.1	.00064
73	.409	856	476	13.2	7.34	.333	6,800	.00369	75.4	.00062
74	.388	810	450	11.7	6.51	.330	6,740	.00314	64.0	.00053
75	.375	783	435	10.6	5.89	.327	6,680	.00275	56.2	.00046
76	.360	752	418	9.9	5.50	.324	6,620	.00249	50.9	.00042
77	.355	741	412	9.3	5.17	.324	6,620	.00230	47.1	.00039
78	.418	872	485	13.3	7.39	.188	3,840	.00222	45.3	.00037
79	.409	856	476	11.7	6.51	.188	3,840	.00194	39.6	.00033
80	-----	----	---	----	-----	-----	------	-------	-----	-------
81	.521	1089	605	13.0	7.23	.218	4,450	.00332	67.7	.00055
82	.532	1113	619	9.4	5.23	.220	4,490	.00267	54.6	.00045
83	.570	1192	663	14.0	7.78	.224	4,570	.00428	87.4	.00071
84	.514	1075	598	16.8	9.34	.230	4,700	.00427	87.1	.00071
85	.510	1067	593	16.9	9.40	.228	4,660	.00421	85.9	.00070
86	.511	1069	594	15.9	8.84	.228	4,660	.00399	81.5	.00067
87	.499	1043	580	15.9	8.84	.228	4,660	.00386	78.8	.00064
88	.468	980	545	13.9	7.73	.224	4,570	.00309	63.1	.00052
89	.474	991	551	13.3	7.39	.225	4,600	.00296	60.4	.00049
90	.451	942	524	12.4	6.89	.222	4,530	.00262	53.5	.00044
91	.448	937	521	11.8	6.56	.199	4,060	.00223	45.5	.00037
92	.455	952	529	12.8	7.12	.199	4,060	.00249	50.9	.00042

TABLE VII. – HEAT-TRANSFER MEASUREMENTS ON FLIGHT 2-22 - Continued

(c) Wing lower surface

Thermo-couple	$\frac{T_w}{T_R}$	T_w,		$\frac{dT_w}{dt}$,		$\rho_w c_{p,w} \tau$,		h_T,		$N_{St,\infty}$
		°R	°K	R° per sec	K° per sec	$\frac{Btu}{ft^2\text{-}°R}$	$\frac{J}{m^2\text{-}°K}$	$\frac{Btu}{ft^2\text{-}sec\text{-}°R}$	$\frac{J}{m^2\text{-}sec\text{-}°K}$	
93	0.445	931	518	11.5	6.39	0.372	7,600	0.00392	80.0	0.00065
94	.503	1052	585	9.9	5.50	.382	7,800	.00405	82.8	.00068
95	.508	1062	590	18.3	10.17	.382	7,800	.00724	147.8	.00121
96	.464	971	540	15.1	8.40	.375	7,660	.00534	109.0	.00089
97	.444	929	517	14.0	7.78	.372	7,600	.00469	95.8	.00078
98	.430	900	500	13.5	7.51	.368	7,520	.00436	89.0	.00073
99	.420	879	489	11.7	6.51	.316	6,450	.00322	65.7	.00054
100	.417	871	484	12.3	6.84	.316	6,450	.00335	68.4	.00056
101	.407	852	474	10.8	6.00	.316	6,450	.00290	59.3	.00049
102	.412	861	479	11.7	6.51	.316	6,450	.00317	64.7	.00053
103	.375	784	436	8.8	4.89	.311	6,350	.00219	44.8	.00037
104	.367	766	426	8.7	4.84	.308	6,290	.00210	42.9	.00035
105	.375	783	435	8.8	4.89	.311	6,350	.00220	45.0	.00037
106	.390	815	453	8.8	4.89	.187	3,820	.00142	29.0	.00024
107	.402	841	468	9.3	5.17	.189	3,860	.00154	31.5	.00026
108	.654	1370	762	29.5	16.40	.328	6,700	.01504	307.2	.00248
109	.612	1282	713	24.5	13.62	.320	6,530	.01083	221.2	.00179
110	.570	1193	663	22.8	12.68	.316	6,450	.00859	175.5	.00143
111	.521	1089	605	20.8	11.56	.308	6,290	.00688	140.4	.00115
112	.505	1060	589	19.5	10.84	.277	5,660	.00562	114.8	.00094
113	.492	1030	573	18.0	10.01	.276	5,640	.00505	103.0	.00084
114	.472	987	549	16.6	9.23	.272	5,550	.00439	89.7	.00073
115	.476	995	553	16.8	9.34	.273	5,580	.00450	91.8	.00075
116	.469	981	545	16.0	8.90	.272	5,550	.00419	85.6	.00070
117	.451	943	524	14.6	8.12	.270	5,510	.00368	75.1	.00061
118	.427	893	497	13.3	7.39	.268	5,470	.00316	64.6	.00053
119	.407	852	474	11.9	6.62	.265	5,410	.00270	55.2	.00045
120	.425	888	494	12.5	6.95	.189	3,860	.00215	44.0	.00036
121	.426	891	495	12.2	6.78	.189	3,860	.00211	43.2	.00035
122	.514	1076	598	11.3	6.28	.224	4,570	.00296	60.5	.00049
123	.631	1321	734	22.5	12.51	.237	4,840	.00830	169.5	.00137
124	.614	1286	715	21.8	12.12	.227	4,640	.00732	149.5	.00121
125	.593	1242	691	17.7	9.84	.227	4,640	.00571	116.7	.00095
126	.590	1236	687	16.5	9.17	.226	4,620	.00531	108.4	.00088
127	.556	1164	647	17.2	9.56	.222	4,530	.00480	98.0	.00080
128	.569	1191	662	17.6	9.79	.226	4,620	.00519	105.9	.00086
129	.524	1096	609	16.5	9.17	.218	4,450	.00413	84.3	.00069
130	.528	1105	614	15.7	8.73	.220	4,490	.00402	82.1	.00067
131	.491	1027	571	14.4	8.01	.214	4,370	.00327	66.7	.00055
132	.477	997	554	13.2	7.34	.202	4,130	.00273	55.8	.00046
133	.471	986	548	13.3	7.39	.202	4,130	.00274	56.0	.00046
134	.456	954	530	12.5	6.95	.200	4,080	.00243	49.6	.00041

TABLE VII. – HEAT-TRANSFER MEASUREMENTS ON FLIGHT 2-22 - Continued

(d) Horizontal-tail upper surface

Thermocouple	$\frac{T_w}{T_R}$	T_w,		$\frac{dT_w}{dt}$,		$\rho_w c_{p,w} \tau$,		h_T,		$N_{St,\infty}$
		°R	°K	R° per sec	K° per sec	$\frac{Btu}{ft^2-°R}$	$\frac{J}{m^2-°K}$	$\frac{Btu}{ft^2-sec-°R}$	$\frac{J}{m^2-sec-°K}$	
135	0.578	1210	673	22.4	12.45	0.266	5,430	0.00761	155.3	0.00126
136	.498	1042	579	14.8	8.23	.256	5,230	.00401	81.8	.00067
137	.473	989	550	13.1	7.28	.253	5,170	.00331	67.6	.00055
138	.509	1065	592	17.5	9.73	.258	5,270	.00484	98.8	.00081
139	.431	902	502	11.7	6.51	.249	5,090	.00265	54.0	.00044
140	.429	898	499	11.6	6.45	.243	4,960	.00255	52.0	.00043
141	.430	900	500	12.6	7.01	.249	5,090	.00283	57.8	.00047

(e) Horizontal-tail lower surface

Thermocouple	$\frac{T_w}{T_R}$	T_w,		$\frac{dT_w}{dt}$,		$\rho_w c_{p,w} \tau$,		h_T,		$N_{St,\infty}$
		°R	°K	R° per sec	K° per sec	$\frac{Btu}{ft^2-°R}$	$\frac{J}{m^2-°K}$	$\frac{Btu}{ft^2-sec-°R}$	$\frac{J}{m^2-sec-°K}$	
142	0.539	1128	627	16.1	8.95	0.262	5,350	0.00497	101.4	0.00083
143	.476	995	553	11.1	6.17	.253	5,170	.00288	58.8	.00048
144	.511	1068	594	15.2	8.45	.258	5,270	.00428	87.3	.00071
145	.453	947	527	13.2	7.34	.251	5,130	.00315	64.3	.00053
146	.402	841	468	9.6	5.34	.245	5,000	.00203	41.4	.00034
147	.405	846	470	9.3	5.17	.245	5,000	.00198	40.5	.00033

TABLE VII. – HEAT-TRANSFER MEASUREMENTS ON FLIGHT 2-22 - Continued

(f) Vertical tail

Thermocouple	$\frac{T_w}{T_R}$	T_w,		$\frac{dT_w}{dt}$,		$\rho_w c_{p,w} \tau$,		h_T,		$N_{St,\infty}$
		°R	°K	R° per sec	K° per sec	$\frac{Btu}{ft^2\text{-}°R}$	$\frac{J}{m^2\text{-}°K}$	$\frac{Btu}{ft^2\text{-}sec\text{-}°R}$	$\frac{J}{m^2\text{-}sec\text{-}°K}$	
148	0.354	740	411	8.3	4.61	0.447	9,130	0.00282	57.7	0.00048
149	.413	864	480	8.3	4.61	.338	6,900	.00244	49.8	.00041
150	.597	1250	695	21.9	12.18	.200	4,080	.00622	127.0	.00103
151	.550	1151	640	17.7	9.84	.193	3,940	.00429	87.6	.00071
152	.628	1315	731	16.1	8.95	.109	2,230	.00360	73.5	.00060
153	.574	1202	668	16.2	9.01	.106	2,170	.00276	56.4	.00046
154	-----	----	---	----	-----	-----	------	-------	-----	-------
155	.557	1165	648	17.1	9.51	.105	2,140	.00264	53.9	.00044
156	-----	----	---	----	-----	-----	------	-------	-----	-------
157	.570	1192	663	16.9	9.40	.106	2,170	.00279	56.9	.00046
158	.343	717	399	10.1	5.62	.625	12,760	.00466	95.2	.00079
159	.357	747	415	9.7	5.39	.610	12,460	.00448	91.5	.00076
160	-----	----	---	----	-----	-----	------	-------	-----	-------
161	.375	784	436	10.5	5.84	.514	10,500	.00425	86.8	.00072
162	.375	783	435	11.3	6.28	.460	9,390	.00408	83.3	.00069
163	.396	827	460	11.7	6.51	.421	8,600	.00404	82.5	.00068
164	.395	825	459	10.3	5.73	.480	9,800	.00403	82.4	.00068
[a]164L	.327	684	380	3.2	1.78	.462	9,430	.00112	22.9	.00019
165	.446	933	519	12.5	6.95	.389	7,940	.00442	90.2	.00074
165L	.449	939	522	11.9	6.62	.388	7,920	.00423	86.4	.00071
166	.583	1220	678	17.8	9.90	.197	4,020	.00476	97.2	.00079
166L	.568	1189	661	16.5	9.17	.196	4,000	.00437	89.2	.00073
167	-----	----	---	----	-----	-----	------	-------	-----	-------
167L	.572	1197	666	16.6	9.23	.196	4,000	.00443	90.4	.00074
168	-----	----	---	----	-----	-----	------	-------	-----	-------
168L	.571	1196	665	18.4	10.23	.196	4,000	.00483	98.5	.00080
169L	.544	1138	633	16.6	9.23	.193	3,940	.00397	81.1	.00066
170	.529	1108	616	14.6	8.12	.157	3,210	.00287	58.6	.00048
170L	.524	1096	609	14.1	7.84	.156	3,190	.00271	55.4	.00045
171	.591	1237	688	19.2	10.68	.160	3,270	.00455	92.9	.00075
171L	.579	1212	674	18.8	10.45	.159	3,250	.00425	86.9	.00071
172	.554	1160	645	16.7	9.29	.158	3,230	.00351	71.6	.00058
172L	-----	----	---	----	-----	-----	------	-------	-----	-------
173	.530	1110	617	15.4	8.56	.157	3,210	.00303	61.9	.00051
174	.532	1114	619	15.0	8.34	.157	3,210	.00296	60.5	.00049
174L	.581	1217	677	19.6	10.90	.160	3,270	.00447	91.3	.00074
175	.401	839	466	11.2	6.23	.416	8,500	.00388	79.2	.00065
176	.570	1192	663	17.8	9.90	.197	4,020	.00468	95.6	.00078
177	.538	1125	626	14.5	8.06	.194	3,960	.00350	71.5	.00058
178	.527	1103	613	13.5	7.51	.194	3,960	.00317	64.7	.00053
179	.552	1155	642	15.6	8.67	.195	3,980	.00391	79.8	.00065
180	.529	1107	615	14.3	7.95	.194	3,960	.00335	68.3	.00056

[a]L indicates thermocouple on left side.

TABLE VII. – HEAT-TRANSFER MEASUREMENTS ON FLIGHT 2-22 - Concluded

(g) Ventral tail

Thermocouple	$\frac{T_w}{T_R}$	T_w,		$\frac{dT_w}{dt}$,		$\rho_w c_{p,w} \tau$,		h_T,		$N_{St,\infty}$
		°R	°K	R° per sec	K° per sec	$\frac{Btu}{ft^2\text{-}°R}$	$\frac{J}{m^2\text{-}°K}$	$\frac{Btu}{ft^2\text{-}sec\text{-}°R}$	$\frac{J}{m^2\text{-}sec\text{-}°K}$	
181	0.405	847	471	10.5	5.84	0.460	9,390	0.00403	82.2	0.00068
182	.506	1059	589	15.1	8.40	.372	7,600	.00586	119.6	.00098
183	.584	1224	681	19.4	10.79	.198	4,040	.00533	108.8	.00088
184	.549	1149	639	17.3	9.62	.195	3,980	.00424	86.5	.00070
185	.628	1315	731	16.4	9.12	.109	2,230	.00364	74.4	.00060
186	.591	1237	688	16.6	9.23	.108	2,210	.00306	62.5	.00051
187	.628	1315	731	15.9	8.84	.109	2,230	.00358	73.1	.00059
188	.594	1243	691	17.5	9.73	.109	2,230	.00324	66.1	.00054
189	.573	1200	667	12.7	7.06	.107	2,190	.00234	47.8	.00039
190	.361	754	419	11.0	6.12	.630	12,870	.00527	107.6	.00089
191	.369	772	429	10.5	5.84	.610	12,460	.00497	101.6	.00084

TABLE VIII. – HEAT-TRANSFER MEASUREMENTS ON FLIGHT 2-28

(a) Fuselage

Thermo-couple	$\frac{T_w}{T_R}$	T_w,		$\frac{dT_w}{dt}$,		$\rho_w c_{p,w} \tau$,		h_T,		$N_{St,\infty}$
		°R	°K	R° per sec	K° per sec	$\frac{Btu}{ft^2-°R}$	$\frac{J}{m^2-°K}$	$\frac{Btu}{ft^2-sec-°R}$	$\frac{J}{m^2-sec-°K}$	
1	0.464	961	534	23.1	12.84	0.684	13,970	0.01452	296.5	0.00452
2	.483	1000	556	21.6	12.01	.619	12,640	.01280	261.4	.00398
3	.447	924	514	16.3	9.06	.451	9,210	.00665	135.8	.00207
4	.435	901	501	9.7	5.39	.394	8,040	.00347	70.9	.00108
5	.410	849	472	3.5	1.95	.390	7,960	.00127	25.9	.00040
6	.410	848	471	4.0	2.22	.390	7,960	.00144	29.4	.00045
7	.455	942	524	10.7	5.95	.396	8,090	.00401	81.9	.00125
8	.395	818	455	2.3	1.28	.342	6,980	.00075	15.3	.00023
9	.471	974	542	11.7	6.51	.354	7,230	.00407	83.1	.00127
10	.513	1063	591	24.6	13.68	.386	7,880	.00989	202.0	.00307
11	.490	1015	564	17.6	9.79	.361	7,370	.00638	130.3	.00198
12	.419	866	481	5.5	3.06	.286	5,840	.00148	30.2	.00046
13	.399	826	459	2.1	1.17	.284	5,800	.00062	12.7	.00020
14	.474	982	546	11.0	6.12	.294	6,000	.00329	67.2	.00102
15	.254	524	291	2.0	1.11	.221	4,510	.00031	6.3	.00010
16	.459	950	528	6.1	3.39	.627	12,800	.00366	74.7	.00114
17	.551	1142	635	24.0	13.34	.282	5,760	.00793	161.9	.00246
18	.540	1118	622	19.4	10.79	.282	5,760	.00633	129.3	.00196
19	.465	963	535	11.9	6.62	.273	5,580	.00321	65.6	.00100
20	.411	851	473	4.3	2.39	.247	5,040	.00102	20.8	.00032
21	.439	909	505	4.6	2.56	.620	12,660	.00264	53.9	.00082
22	.449	930	517	8.6	4.78	.272	5,550	.00228	46.6	.00071
23	.457	945	525	.8	.44	.590	12,050	.00066	13.5	.00021
24	.553	1145	637	23.9	13.29	.271	5,530	.00764	156.0	.00237
25	.518	1073	597	20.5	11.40	.267	5,450	.00594	121.3	.00185
26	.392	811	451	4.0	2.22	.244	4,980	.00090	18.4	.00028
27	.390	806	448	7.0	3.89	.244	4,980	.00148	30.2	.00046
28	.411	850	473	5.7	3.17	.245	5,000	.00130	26.6	.00041
29	.441	912	507	10.8	6.00	.285	5,270	.00263	53.7	.00082
30	.459	950	528	19.1	10.62	.260	5,310	.00470	96.0	.00146
31	.428	886	493	13.8	7.67	.258	5,270	.00319	65.1	.00100
32	.342	707	393	1.9	1.06	.247	5,040	.00041	8.4	.00013
33	.274	566	315	2.4	1.33	.224	4,570	.00038	7.8	.00012
34	.393	814	453	4.3	2.39	.357	7,290	.00136	27.8	.00043
35	.440	910	506	16.5	9.17	.258	5,270	.00387	79.0	.00121
36	.439	908	505	13.7	7.62	.258	5,270	.00325	66.4	.00101
37	.437	904	503	13.7	7.62	.258	5,270	.00325	66.4	.00101
38	.529	1096	609	16.2	9.01	.192	3,920	.00371	75.8	.00115
39	.438	906	504	6.8	3.78	.184	3,760	.00128	26.1	.00040
40	.265	547	304	1.0	.56	.576	11,760	.00040	8.2	.00013
41	.285	590	328	1.8	1.00	.287	5,860	.00037	7.6	.00012
42	.317	656	365	1.6	.89	.300	6,130	.00040	8.2	.00013
43	-----	----	---	----	-----	-----	------	-------	-----	-------
44	.613	1270	706	20.8	11.56	.126	2,570	.00441	90.1	.00136
45	.385	797	443	-.9	-.50	.114	2,330	.00003	.6	.00001
46	.340	704	391	1.3	.72	.114	2,330	.00018	3.7	.00006
47	-----	----	---	----	-----	-----	------	-------	-----	-------
48	-----	----	---	----	-----	-----	------	-------	-----	-------
49	.311	644	358	1.9	1.06	.110	2,250	.00019	3.9	.00006
50	.365	756	420	3.8	2.11	.112	2,290	.00041	8.4	.00013

TABLE VIII. – HEAT-TRANSFER MEASUREMENTS ON FLIGHT 2-28 - Continued

(b) Wing upper surface

Thermo-couple	$\frac{T_w}{T_R}$	T_w,		$\frac{dT_w}{dt}$,		$\rho_w c_{p,w} \tau$,		h_T,		$N_{St,\infty}$
		°R	°K	R° per sec	K° per sec	$\frac{Btu}{ft^2\text{-}°R}$	$\frac{J}{m^2\text{-}°K}$	$\frac{Btu}{ft^2\text{-}sec\text{-}°R}$	$\frac{J}{m^2\text{-}sec\text{-}°K}$	
51	0.321	663	369	4.2	2.34	0.326	6,660	0.00101	20.6	0.00032
52	.311	644	358	3.6	2.00	.326	6,660	.00086	17.6	.00027
53	.323	667	371	2.4	1.33	.322	6,580	.00061	12.5	.00019
54	.341	706	393	.4	.22	.318	6,490	.00016	3.3	.00005
55	.342	708	394	.2	.11	.314	6,410	.00010	2.0	.00003
56	.295	610	339	.2	.11	.404	8,250	.00009	1.8	.00003
57	-----	----	---	----	-----	-----	------	-------	-----	-------
58	.298	617	343	.5	.28	.404	8,250	.00017	3.5	.00006
59	.300	620	447	1.4	.78	.407	8,310	.00042	8.6	.00013
60	.278	575	320	1.7	.95	.396	8,090	.00047	9.6	.00015
61	.271	560	311	1.2	.67	.396	8,090	.00035	7.2	.00011
62	.277	573	319	1.1	.61	.396	8,090	.00032	6.5	.00010
63	.330	682	379	1.1	.61	.180	3,680	.00020	4.1	.00006
64	.332	687	382	1.8	1.00	.180	3,680	.00029	5.9	.00009
65	.336	694	386	2.4	1.33	.180	3,680	.00037	7.6	.00012
66	.368	762	424	8.4	4.67	.272	5,550	.00184	37.6	.00058
67	.357	739	411	7.8	4.34	.270	5,510	.00166	33.9	.00052
68	.352	728	405	9.4	5.23	.270	5,510	.00197	40.2	.00062
69	.379	785	436	7.4	4.11	.275	5,620	.00169	34.5	.00053
70	369	763	424	4.5	2.50	.325	6,640	.00120	24.5	.00038
71	.365	754	419	5.6	3.11	.325	6,640	.00146	29.8	.00046
72	.353	731	406	5.0	2.78	.322	6,580	.00127	25.9	.00040
73	.354	732	407	4.9	2.72	.322	6,580	.00125	25.5	.00039
74	.335	693	385	3.6	2.00	.319	6,510	.00089	18.2	.00028
75	.324	669	372	2.8	1.56	.319	6,510	.00070	14.3	.00022
76	.315	651	362	3.3	1.83	.319	6,510	.00078	15.9	.00025
77	.313	647	360	2.7	1.50	.319	6,510	.00066	13.5	.00021
78	.347	718	399	2.2	1.22	.181	3,700	.00036	7.4	.00011
79	.346	715	398	3.3	1.83	.181	3,700	.00051	10.4	.00016
80	.313	647	360	3.5	1.95	.180	3,680	.00049	10.0	.00015
81	.392	810	450	5.5	3.06	.206	4,210	.00102	20.8	.00032
82	.388	802	446	4.9	2.72	.206	4,210	.00090	18.4	.00028
83	.385	796	443	2.9	1.61	.206	4,210	.00058	11.8	.00018
84	.367	759	422	1.8	1.00	.213	4,350	.00038	7.8	.00012
85	.380	787	438	2.5	1.39	.216	4,410	.00053	10.8	.00017
86	.400	827	460	2.1	1.17	.217	4,430	.00050	10.2	.00016
87	.402	832	463	3.5	1.95	.218	4,450	.00076	15.5	.00024
88	.396	820	456	3.6	2.00	.218	4,450	.00076	15.5	.00024
89	.397	822	457	3.7	2.06	.217	4,430	.00077	15.7	.00024
90	.385	797	443	3.8	2.11	.218	4,450	.00077	15.7	.00024
91	.393	814	453	3.6	2.00	.194	3,960	.00066	13.5	.00021
92	.404	836	465	4.3	2.39	.194	3,960	.00081	16.5	.00025

TABLE VIII. – HEAT-TRANSFER MEASUREMENTS ON FLIGHT 2-28 - Continued

(c) Wing lower surface

Thermo-couple	$\frac{T_w}{T_R}$	T_w,		$\frac{dT_w}{dt}$,		$\rho_w c_{p,w} \tau$,		h_T,		$N_{St,\infty}$
		°R	°K	R° per sec	K° per sec	$\frac{Btu}{ft^2-°R}$	$\frac{J}{m^2-°K}$	$\frac{Btu}{ft^2-sec-°R}$	$\frac{J}{m^2-sec-°K}$	
93	0.468	968	538	24.4	13.57	0.375	7,660	0.00857	175.0	0.00267
94	.516	1069	594	30.9	17.18	.385	7,860	.01233	251.8	.00383
95	.540	1119	622	28.3	15.73	.388	7,920	.01212	247.5	.00376
96	.511	1059	589	24.0	13.34	.382	7,800	.00907	185.2	.00295
97	.495	1026	570	24.2	13.46	.378	7,720	.00913	186.4	.00284
98	.482	998	555	24.7	13.73	.375	7,660	.00895	182.8	.00278
99	.480	993	552	19.7	10.96	.324	6,620	.00624	127.4	.00194
100	.486	1006	559	24.9	13.84	.324	6,620	.00792	161.7	.00246
101	.477	987	549	21.2	11.79	.324	6,620	.00667	136.2	.00207
102	.484	1002	557	23.6	13.12	.324	6,620	.00749	153.0	.00233
103	.459	950	528	22.6	12.57	.321	6,560	.00670	136.8	.00209
104	.446	923	513	21.0	11.68	.319	6,510	.00605	123.5	.00189
105	.463	959	533	23.9	13.29	.321	6,560	.00732	149.5	.00222
106	.475	984	547	20.3	11.29	.193	3,940	.00392	80.1	.00122
107	.476	986	548	20.8	11.56	.193	3,940	.00402	82.1	.00125
108	.556	1153	641	29.7	16.51	.314	6,410	.01085	221.6	.00336
109	.589	1220	678	39.7	22.07	.316	6,450	.01562	319.0	.00483
110	.560	1160	645	34.7	19.29	.314	6,410	.01265	258.3	.00392
111	.556	1152	641	31.5	17.51	.313	6,390	.01139	232.6	.00353
112	.563	1166	648	27.1	15.07	.284	5,800	.00923	188.5	.00286
113	.553	1146	637	25.4	14.12	.284	5,800	.00845	172.6	.00262
114	.533	1104	614	25.1	13.96	.282	5,760	.00787	160.7	.00244
115	.537	1112	618	24.4	13.57	.282	5,760	.00773	157.9	.00240
116	.534	1105	614	25.2	14.01	.282	5,760	.00789	161.1	.00245
117	.513	1062	590	23.9	13.29	.278	5,680	.00703	143.6	.00218
118	.485	1004	558	22.3	12.40	.276	5,640	.00610	124.6	.00190
119	.462	956	532	20.6	11.45	.272	5,550	.00528	107.8	.00164
120	.483	999	555	21.5	11.95	.195	3,980	.00423	86.4	.00132
121	.483	999	555	20.5	11.40	.195	3,980	.00406	82.9	.00126
122	.476	985	548	18.1	10.06	.218	4,450	.00395	80.7	.00123
123	.484	1001	557	14.6	8.12	.220	4,490	.00333	68.0	.00103
124	.563	1167	649	7.3	4.06	.222	4,530	.00251	51.3	.00078
125	.615	1275	709	14.8	8.23	.228	4,660	.00539	110.1	.00166
126	.624	1294	719	19.2	10.68	.229	4,680	.00692	141.3	.00213
127	.611	1267	704	22.9	12.73	.227	4,640	.00759	155.0	.00234
128	.617	1280	712	22.6	12.57	.228	4,660	.00770	157.2	.00238
129	.571	1184	658	22.6	12.57	.226	4,620	.00655	133.8	.00203
130	.574	1190	662	21.3	11.84	.226	4,620	.00628	128.2	.00194
131	.544	1126	626	21.9	12.18	.220	4,490	.00569	116.2	.00176
132	.525	1087	604	18.9	10.51	.208	4,250	.00447	91.3	.00139
133	.523	1083	602	19.5	10.84	.208	4,250	.00460	93.9	.00143
134	.506	1048	583	20.8	11.56	.207	4,230	.00458	93.5	.00142

TABLE VIII. – HEAT-TRANSFER MEASUREMENTS ON FLIGHT 2-28 - Continued

(d) Horizontal-tail upper surface

Thermocouple	$\frac{T_w}{T_R}$	T_w,		$\frac{dT_w}{dt}$,		$\rho_w c_{p,w} \tau$,		h_T,		$N_{St,\infty}$
		°R	°K	R° per sec	K° per sec	$\frac{Btu}{ft^2\text{-}°R}$	$\frac{J}{m^2\text{-}°K}$	$\frac{Btu}{ft^2\text{-}sec\text{-}°R}$	$\frac{J}{m^2\text{-}sec\text{-}°K}$	
135	0.637	1320	734	29.6	16.46	0.275	5,620	0.01223	249.7	0.00377
136	.550	1139	633	21.4	11.90	.264	5,390	.00669	136.6	.00207
137	.496	1027	571	16.2	9.01	.256	5,230	.00436	89.0	.00135
138	.523	1084	603	19.1	10.62	.260	5,310	.00553	112.9	.00172
139	.430	890	495	12.6	7.01	.249	5,090	.00285	58.2	.00089
140	.425	880	489	11.9	6.62	.249	5,090	.00268	54.7	.00084
141	-----	----	---	----	-----	-----	------	-------	-----	-------

(e) Horizontal-tail lower surface

Thermocouple	$\frac{T_w}{T_R}$	T_w,		$\frac{dT_w}{dt}$,		$\rho_w c_{p,w} \tau$,		h_T,		$N_{St,\infty}$
		°R	°K	R° per sec	K° per sec	$\frac{Btu}{ft^2\text{-}°R}$	$\frac{J}{m^2\text{-}°K}$	$\frac{Btu}{ft^2\text{-}sec\text{-}°R}$	$\frac{J}{m^2\text{-}sec\text{-}°K}$	
142	0.536	1110	617	23.5	13.07	0.262	5,350	0.00697	142.3	0.00216
143	.458	948	527	14.4	8.01	.251	5,130	.00347	70.9	.00108
144	.504	1044	580	16.7	9.29	.258	5,270	.00461	94.1	.00143
145	.448	927	515	13.5	7.51	.251	5,130	.00321	65.6	.00100
146	.394	816	454	10.0	5.56	.245	5,000	.00208	42.5	.00065
147	.396	819	455	10.7	5.95	.245	5,000	.00222	45.3	.00070

TABLE VIII. – HEAT-TRANSFER MEASUREMENTS ON FLIGHT 2-28 - Continued

(f) Vertical tail

Thermocouple	$\frac{T_w}{T_R}$	T_w,		$\frac{dT_w}{dt}$,		$\rho_w c_{p,w} \tau$,		h_T,		$N_{St,\infty}$
		°R	°K	R° per sec	K° per sec	$\frac{Btu}{ft^2\text{-}°R}$	$\frac{J}{m^2\text{-}°K}$	$\frac{Btu}{ft^2\text{-}sec\text{-}°R}$	$\frac{J}{m^2\text{-}sec\text{-}°K}$	
148	0.290	599	333	3.3	1.83	0.427	8,720	0.00098	20.0	0.00031
149	.307	635	353	2.1	1.17	.333	6,800	.00053	10.8	.00017
150	.382	790	439	1.1	.61	.179	3,660	.00026	5.3	.00008
151	.403	833	463	.9	.50	.177	3,610	.00015	3.1	.00005
152	.493	1020	567	-.5	-.28	.102	2,080	.00032	6.5	.00010
153	.463	958	533	1.1	.61	.101	2,060	.00037	7.6	.00012
154	.297	615	342	-.6	-.33	.092	1,880	.00003	.6	.00001
155	.431	892	496	-1.2	-.67	.100	2,040	.00008	1.6	.00003
156	.411	851	473	-1.5	-.83	.098	2,000	.00003	.6	.00001
157	.425	879	489	-2.2	-1.22	.100	2,040	.00000	0	.00000
158	.298	617	343	2.3	1.28	.602	12,290	.00099	20.2	.00031
159	.303	627	349	1.4	.78	.589	12,030	.00063	12.9	.00020
160	.265	547	304	.7	.39	.505	10,310	.00003	.6	.00008
161	.318	658	366	2.3	1.28	.500	10,210	.00086	17.6	.00027
162	.323	667	371	3.0	1.67	.452	9,230	.00101	20.6	.00032
163	.335	692	385	2.8	1.56	.406	8,290	.00089	18.2	.00028
164	.332	686	381	5.4	3.00	.467	9,540	.00188	38.4	.00059
164L	.311	644	358	1.3	.72	.462	9,430	.00046	9.4	.00015
165	.346	715	398	5.5	3.06	.372	7,600	.00158	32.3	.00050
165L	.360	744	414	5.0	2.78	.375	7,660	.00150	30.7	.00047
166	.480	993	552	4.1	2.28	.187	3,820	.00103	21.0	.00032
166L	.501	1037	577	5.2	2.89	.191	3,900	.00136	27.8	.00042
167	.503	1041	579	6.1	3.39	.191	3,900	.00154	31.5	.00048
167L	.508	1052	585	5.4	3.00	.191	3,900	.00143	29.2	.00044
168	.483	1000	556	5.8	3.22	.189	3,860	.00136	27.8	.00042
168L	.503	1041	579	6.2	3.45	.191	3,900	.00156	31.8	.00048
169L	.479	992	552	4.6	2.56	.188	3,840	.00112	22.8	.00035
170	.475	983	547	5.5	3.06	.152	3,100	.00107	21.9	.00033
170L	.486	1006	559	3.7	2.06	.154	3,150	.00087	17.9	.00027
171	.512	1060	589	6.5	3.61	.155	3,170	.00144	29.5	.00045
171L	-----	----	---	----	-----	-----	------	-------	-----	-------
172	.482	997	554	3.8	2.11	.152	3,100	.00086	17.6	.00027
172L	.354	733	408	1.0	.56	.144	2,940	.00018	3.7	.00006
173	.455	941	523	4.4	2.45	.151	3,080	.00083	16.9	.00026
174	.451	933	519	4.6	2.56	.151	3,080	.00085	17.4	.00027
[a]174L	.478	990	550	2.8	1.56	.152	3,100	.00071	14.5	.00022
175	.328	679	378	2.8	1.56	.401	8,190	.00087	17.8	.00027
176	.494	1024	569	9.3	5.17	.189	3,860	.00206	42.1	.00064
177	.479	992	552	8.3	4.61	.189	3,860	.00177	36.1	.00055
178	.475	983	547	6.7	3.73	.152	3,100	.00125	25.5	.00039
179	.476	986	548	6.6	3.67	.152	3,100	.00124	25.3	.00039
180	.471	975	542	7.1	3.95	.152	3,100	.00127	25.9	.00040

[a]L indicates thermocouple on left side.

TABLE VIII. – HEAT-TRANSFER MEASUREMENTS ON FLIGHT 2-28 - Concluded

(g) Ventral tail

Thermocouple	$\frac{T_w}{T_R}$	T_w,		$\frac{dT_w}{dt}$,		$\rho_w c_{p,w} \tau$,		h_T,		$N_{St,\infty}$
		°R	°K	R° per sec	K° per sec	$\frac{Btu}{ft^2-°R}$	$\frac{J}{m^2-°K}$	$\frac{Btu}{ft^2-sec-°R}$	$\frac{J}{m^2-sec-°K}$	
181	0.382	791	440	11.5	6.39	0.444	9,070	0.00411	83.9	0.00129
182	.446	924	514	16.4	9.12	.347	7,090	.00519	106.0	.00162
183	.598	1239	689	24.5	13.62	.198	4,040	.00681	139.1	.00210
184	.576	1194	664	21.1	11.73	.196	4,000	.00552	112.7	.00171
185	.631	1309	728	18.9	10.51	.109	2,230	.00406	82.9	.00125
186	.601	1246	693	18.4	10.23	.108	2,210	.00343	70.0	.00106
187	.635	1317	732	18.3	10.17	.109	2,230	.00405	82.7	.00125
188	.605	1254	697	22.0	12.23	.108	2,210	.00398	81.3	.00123
189	.584	1210	673	17.7	9.84	.107	2,190	.00308	62.9	.00095
190	.357	739	411	12.5	6.95	.630	12,870	.00600	122.5	.00189
191	.363	752	418	12.2	6.78	.610	12,460	.00574	96.8	.00181

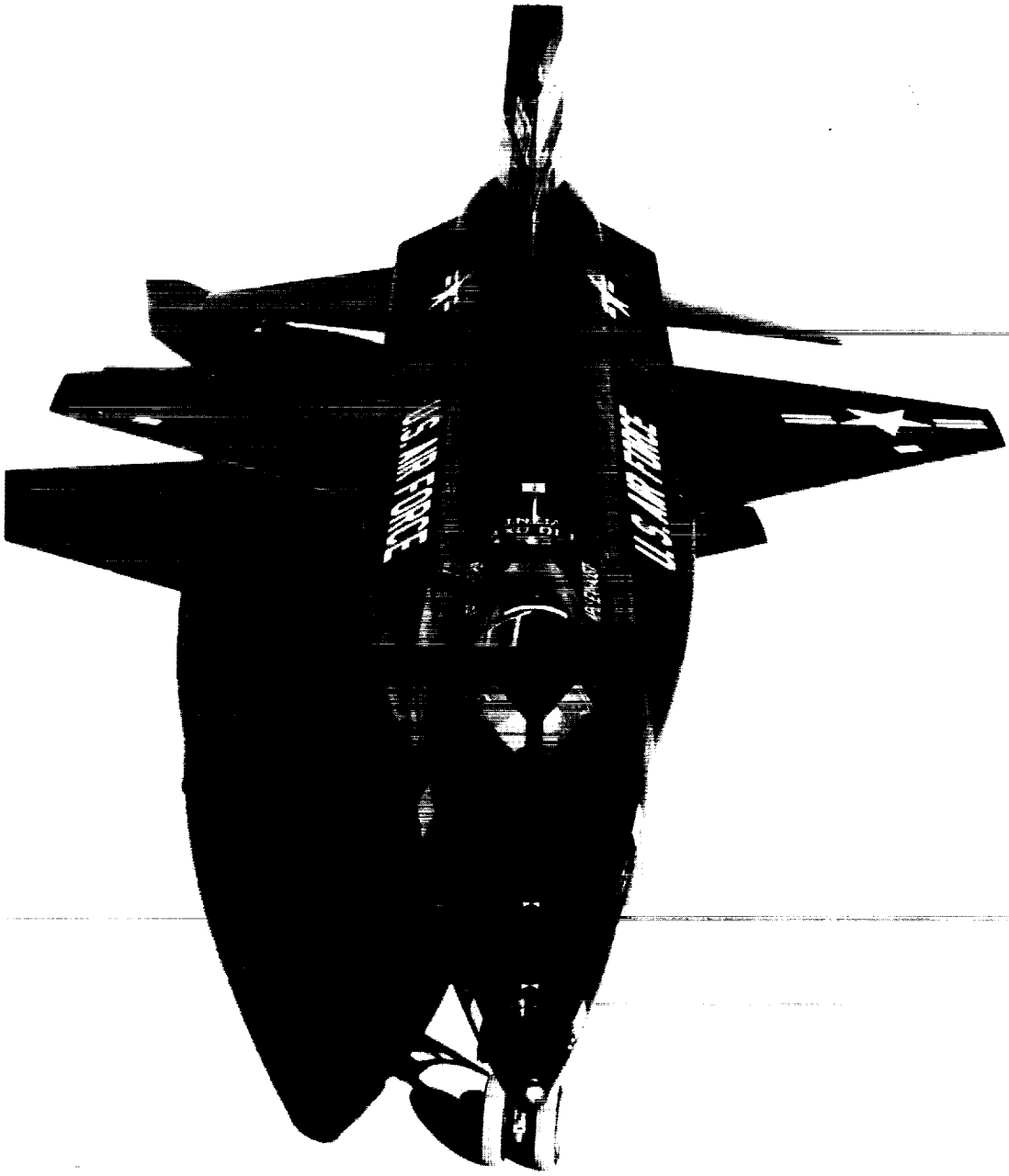

E-7903

Figure 1.– Photograph of the X-15 airplane.

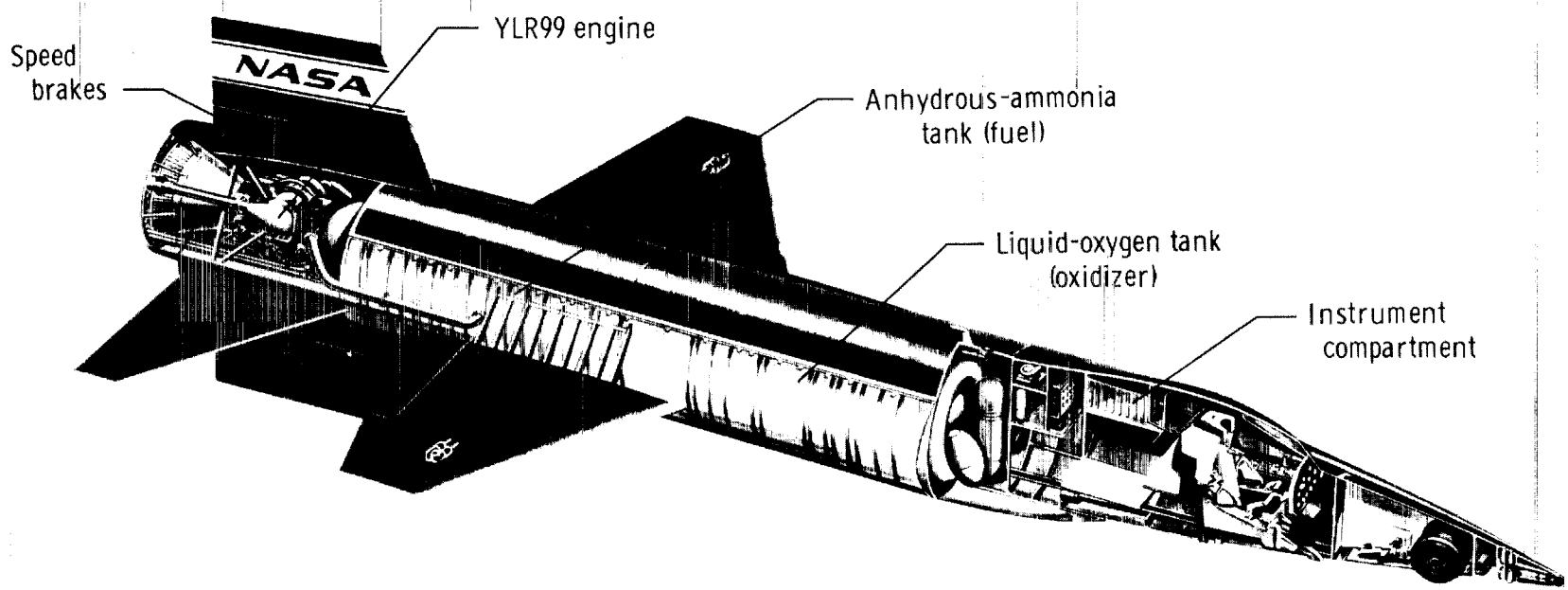

Figure 2. – Cutaway drawing of the X-15 airplane.

E-6990

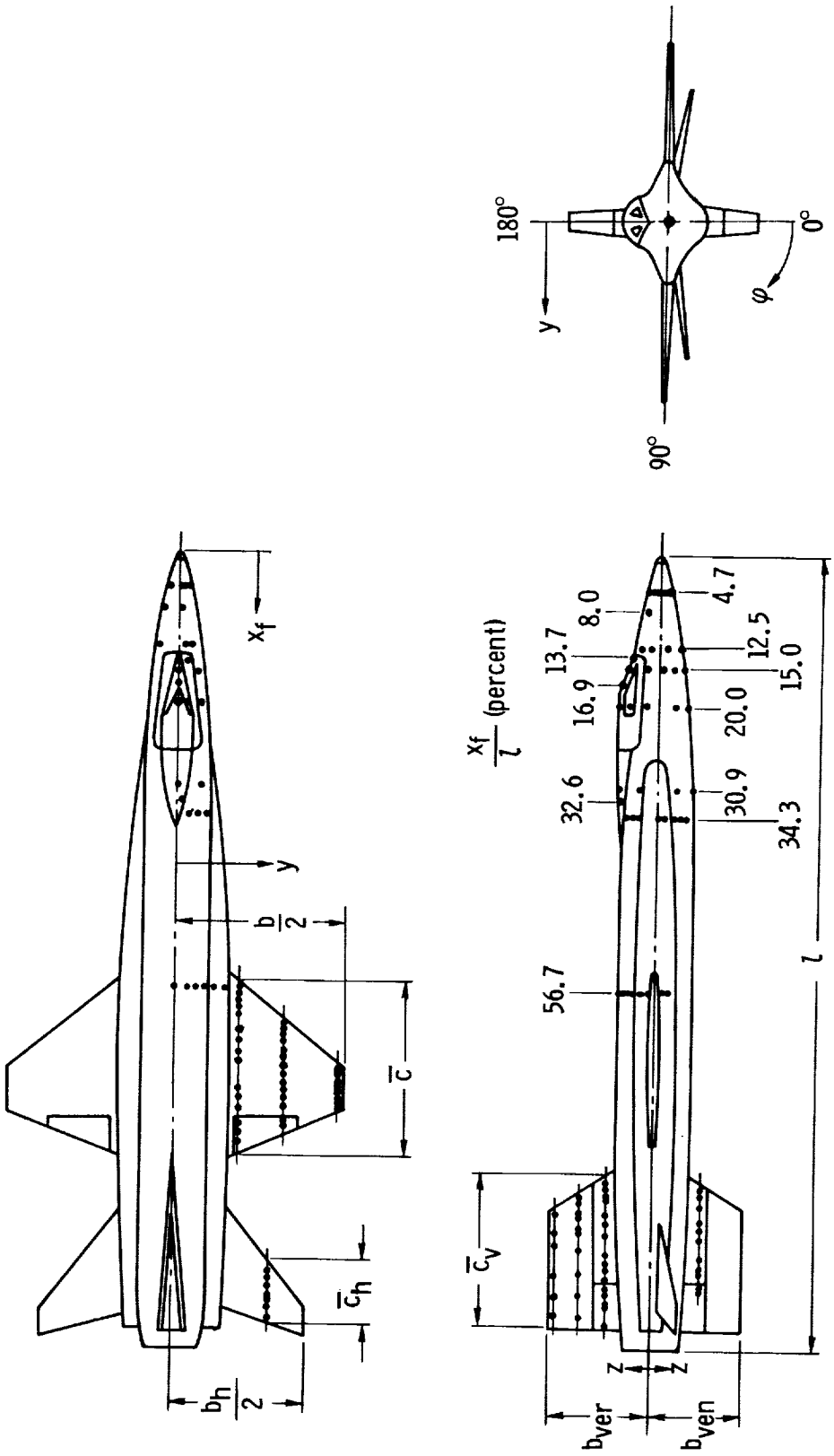

Figure 3. – Thermocouple locations on the X-15 airplane.

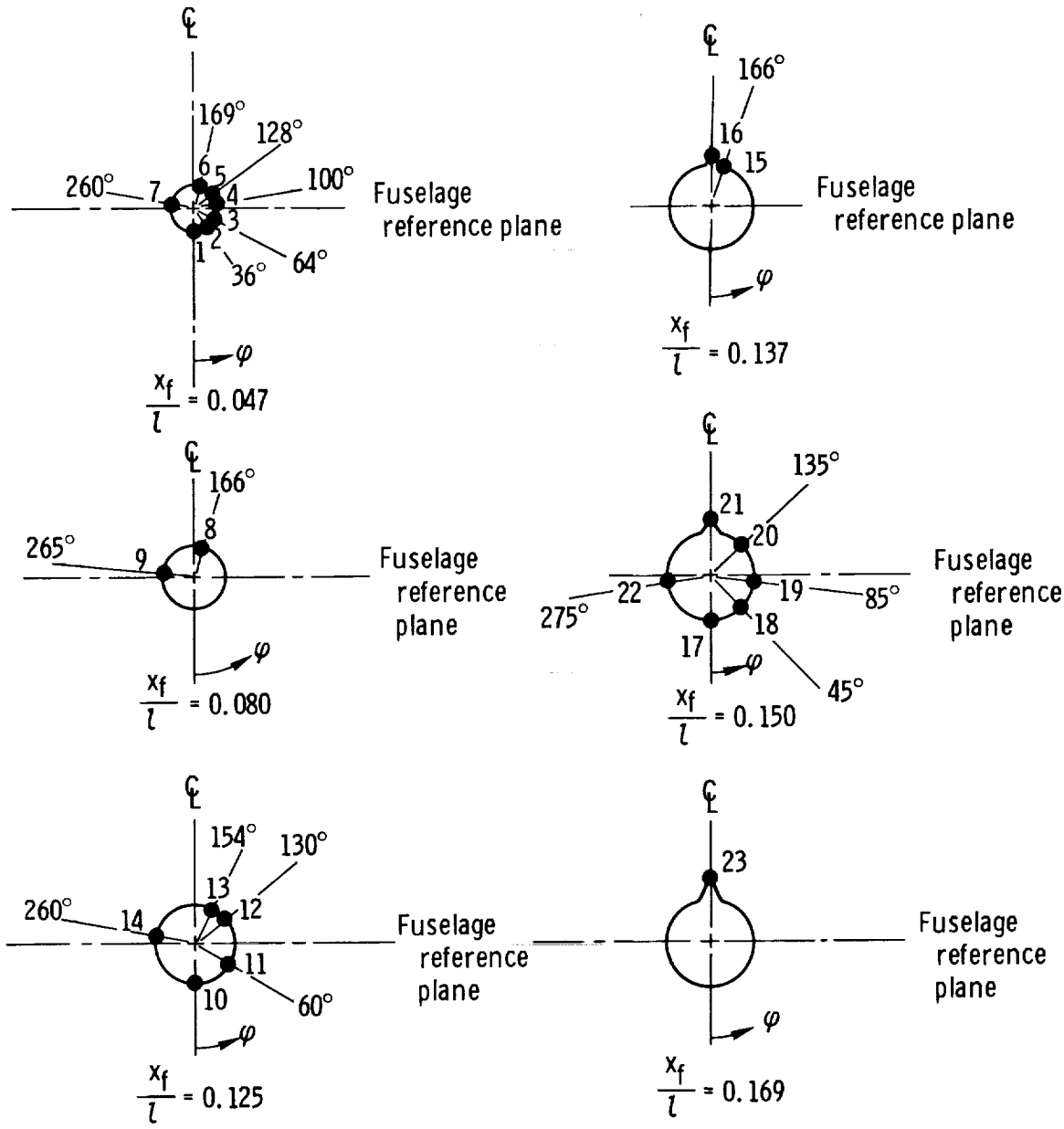

(a) $\frac{x_f}{l}$ = 0.047 to 0.169.

Figure 4.– Fuselage cross sections showing thermocouple locations.

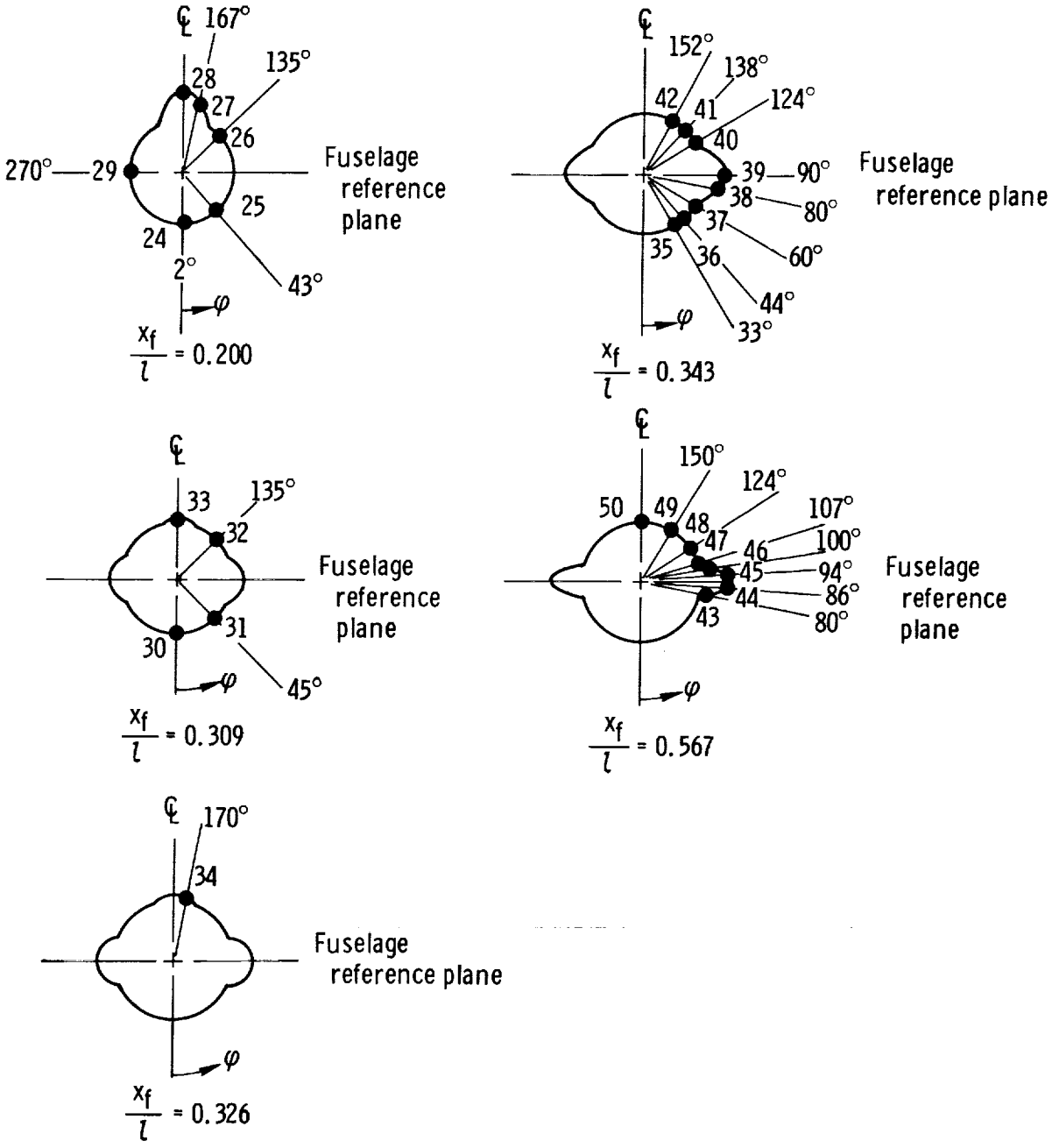

(b) $\frac{x_f}{l}$ = 0.200 to 0.567.

Figure 4. – Concluded.

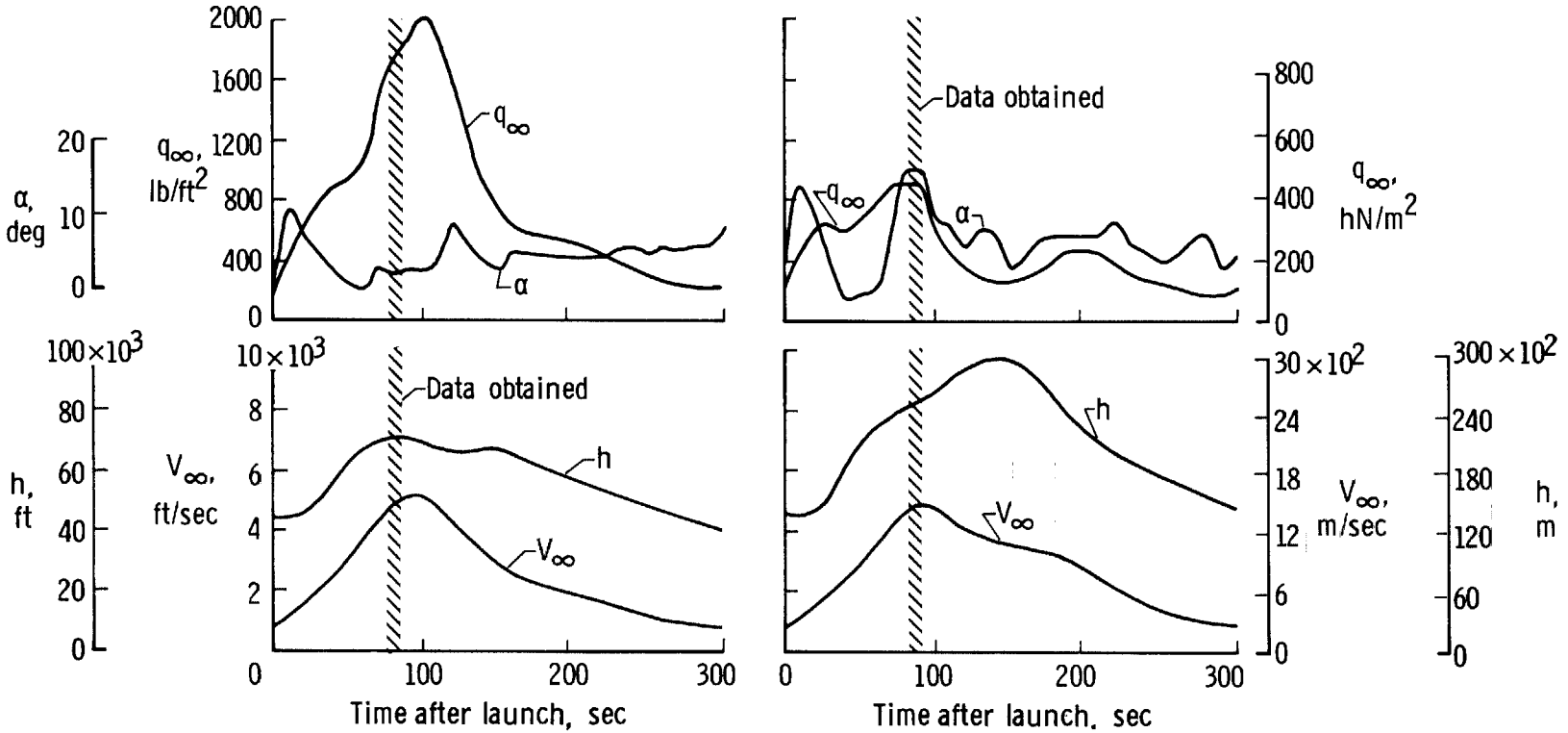

(a) Flight 2-22, low angle of attack.

(b) Flight 2-28, high angle of attack.

Figure 5. – Time histories of flights 2-22 and 2-28.

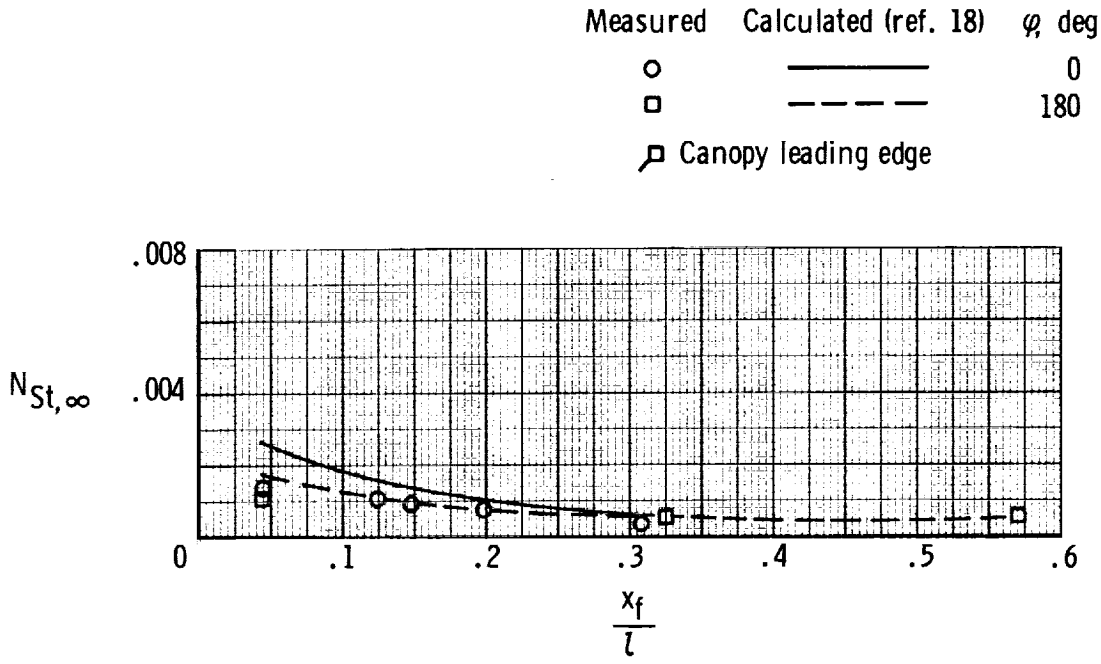

(a) $\alpha = 2.0°$, $M_\infty = 5.10$.

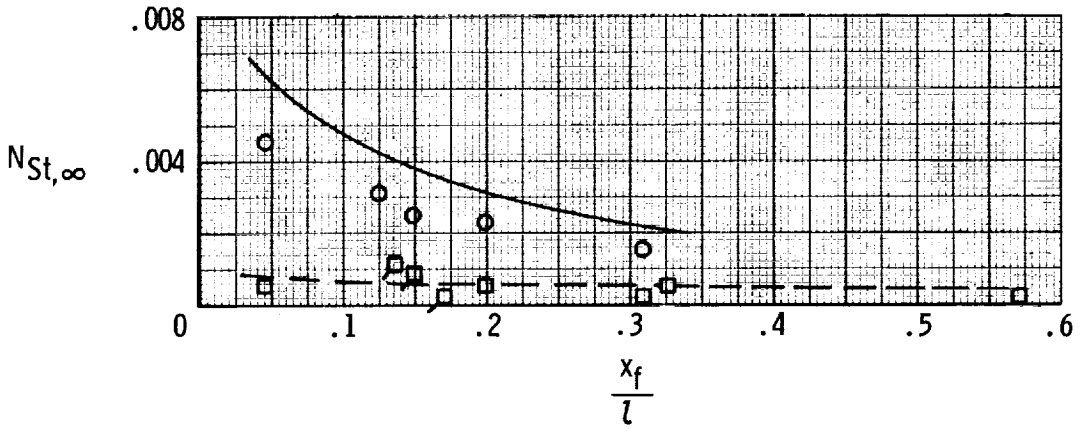

(b) $\alpha = 16.3°$, $M_\infty = 4.98$.

Figure 6. – Effect of angle of attack on distribution of Stanton numbers on vertical center plane of fuselage.

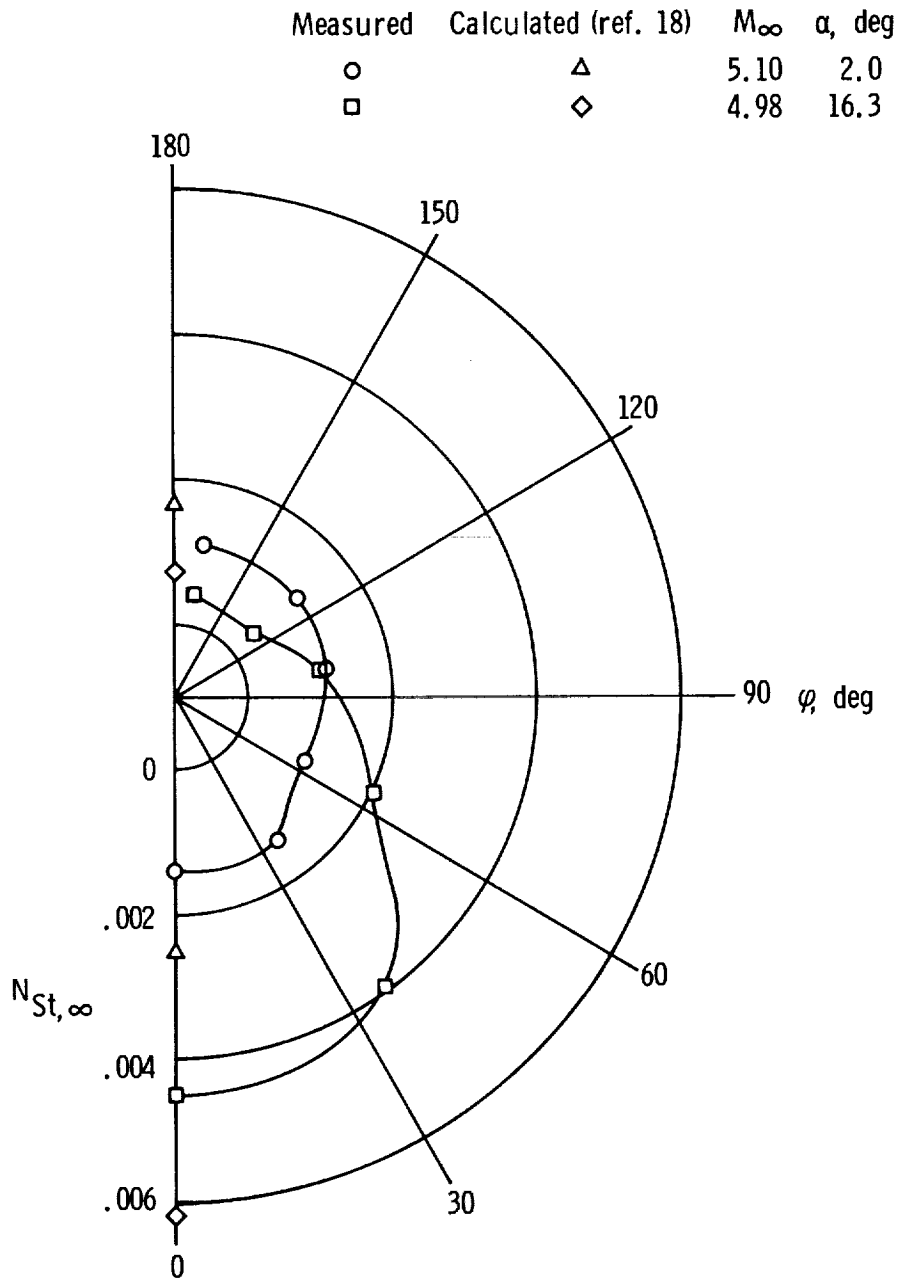

(a) $\frac{x_f}{l} = 0.047$.

Figure 7. – Effect of angle of attack on peripheral distribution of Stanton numbers.

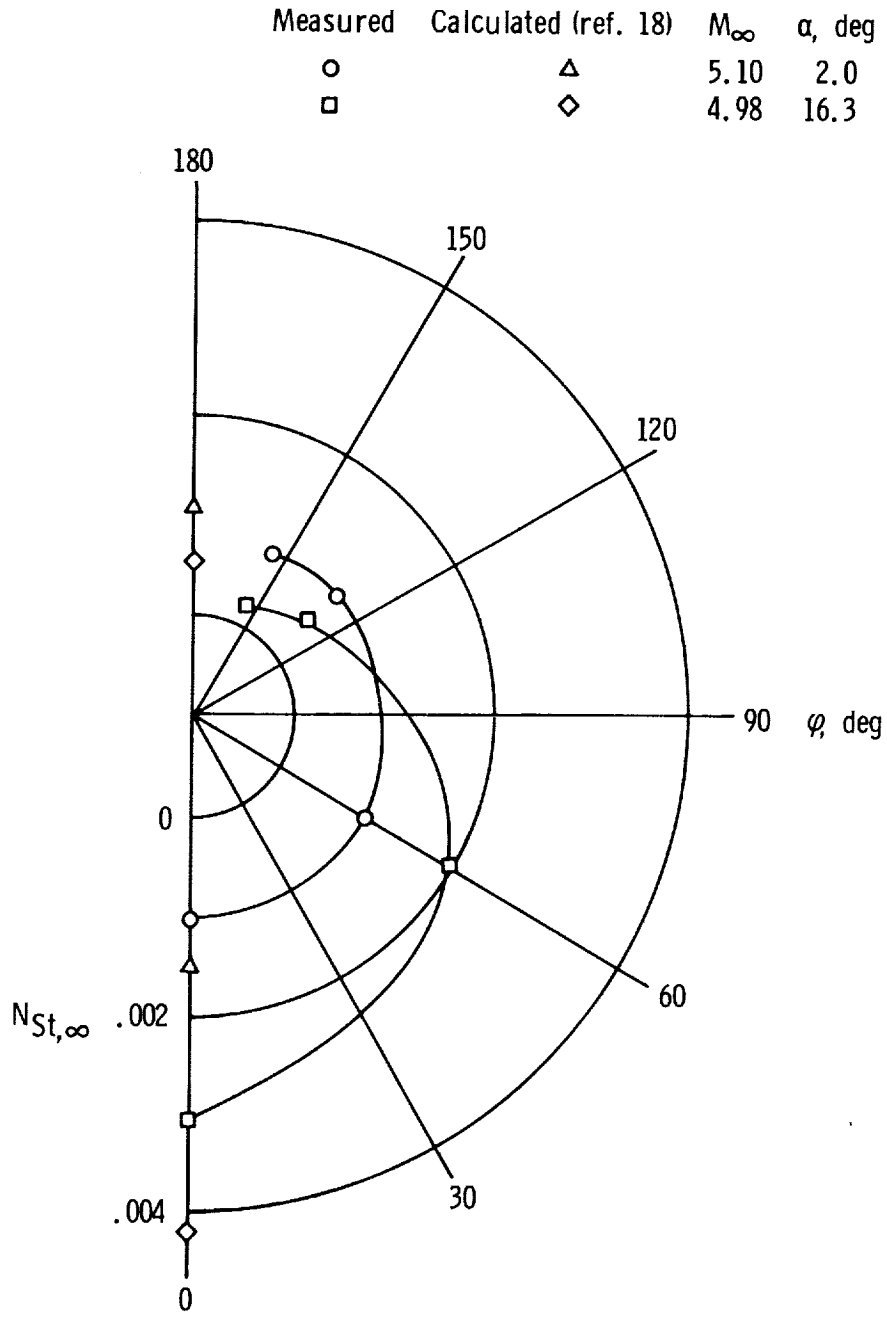

(b) $\frac{x_f}{l} = 0.125$.

Figure 7. – Continued.

Measured	Calculated (ref. 18)	M_∞	α, deg
○	△	5.10	2.0
□	◇	4.98	16.3

Canopy leading edge

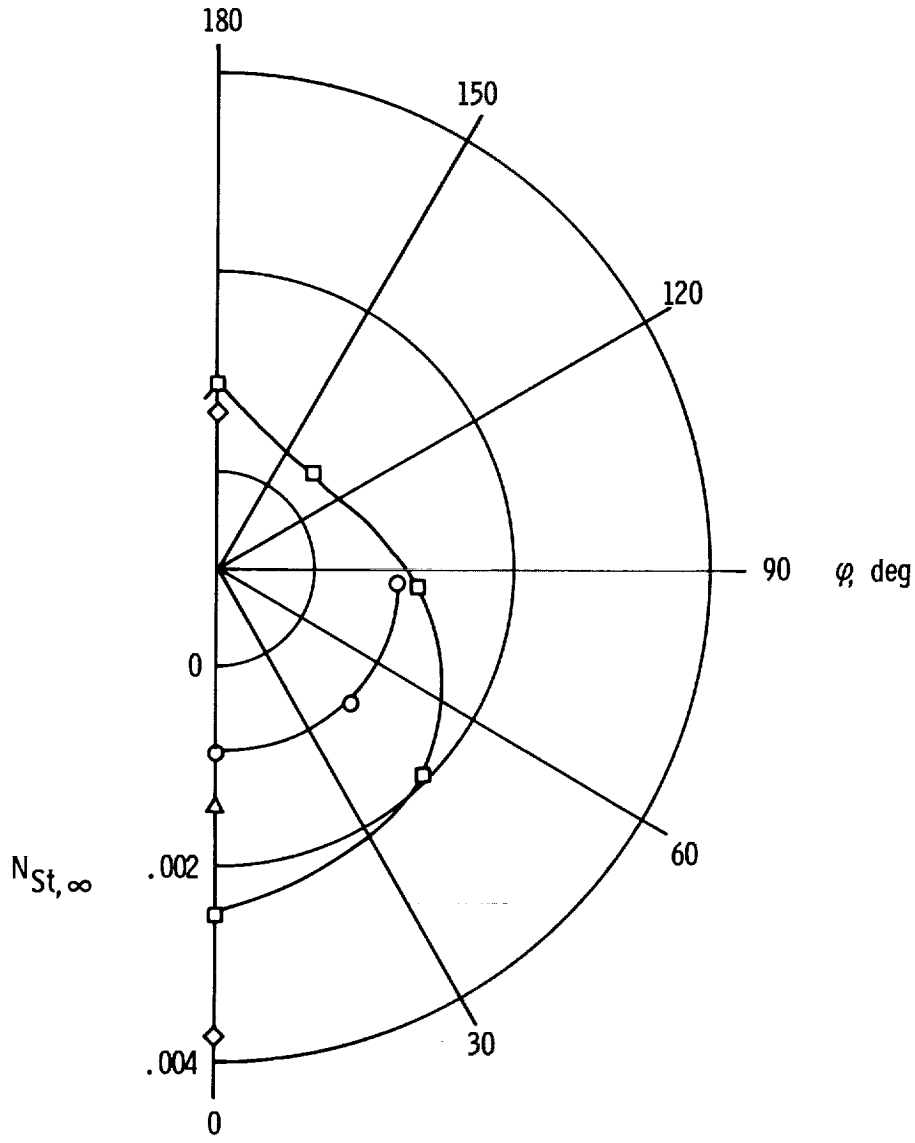

(c) $\frac{x_f}{l} = 0.150$.

Figure 7. – Continued.

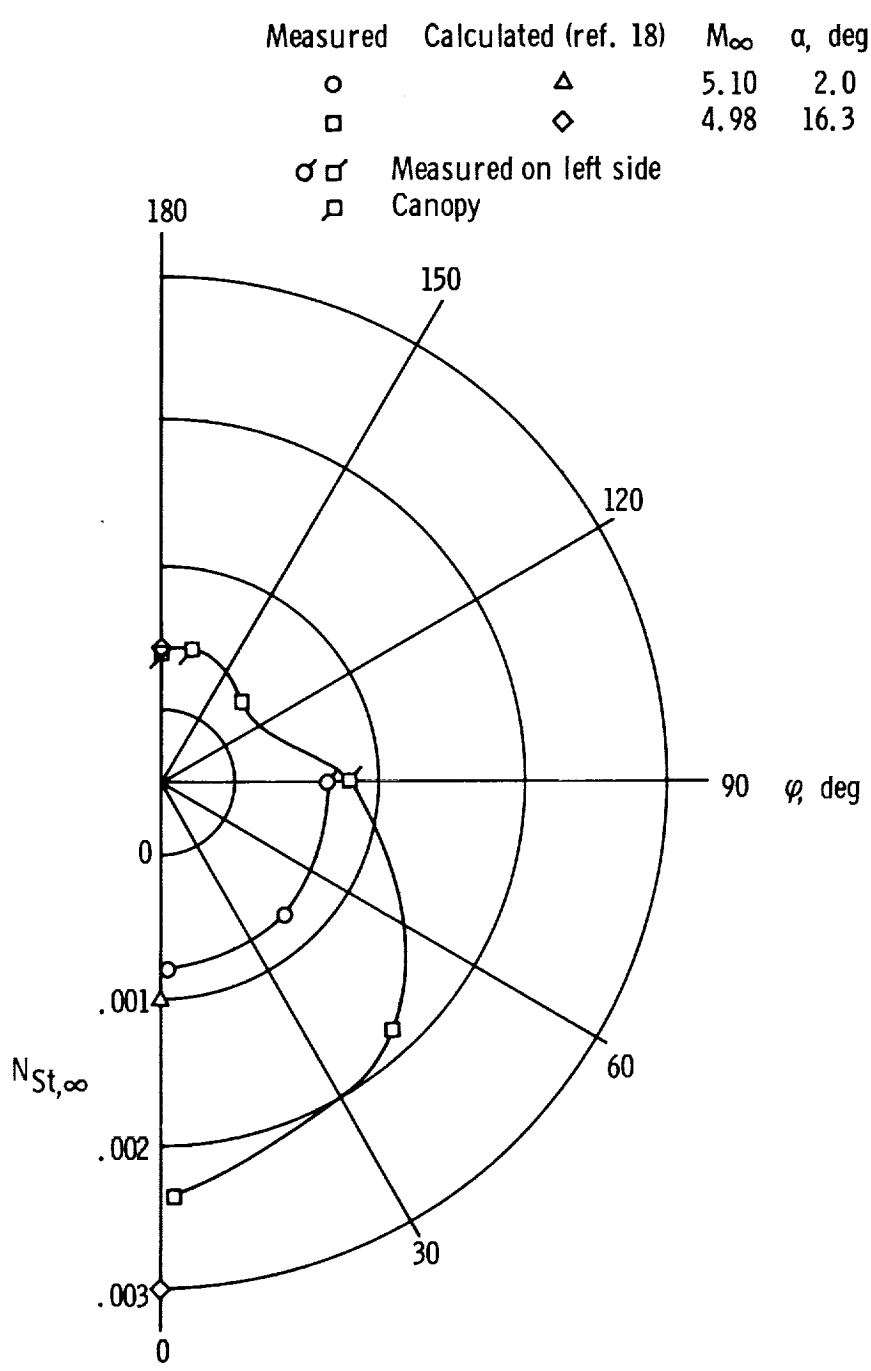

(d) $\frac{x_f}{l} = 0.200$.

Figure 7. – Continued.

Measured	Calculated (ref. 18)	M_∞	α, deg
○	△	5.10	2.0
□	◇	4.98	16.3

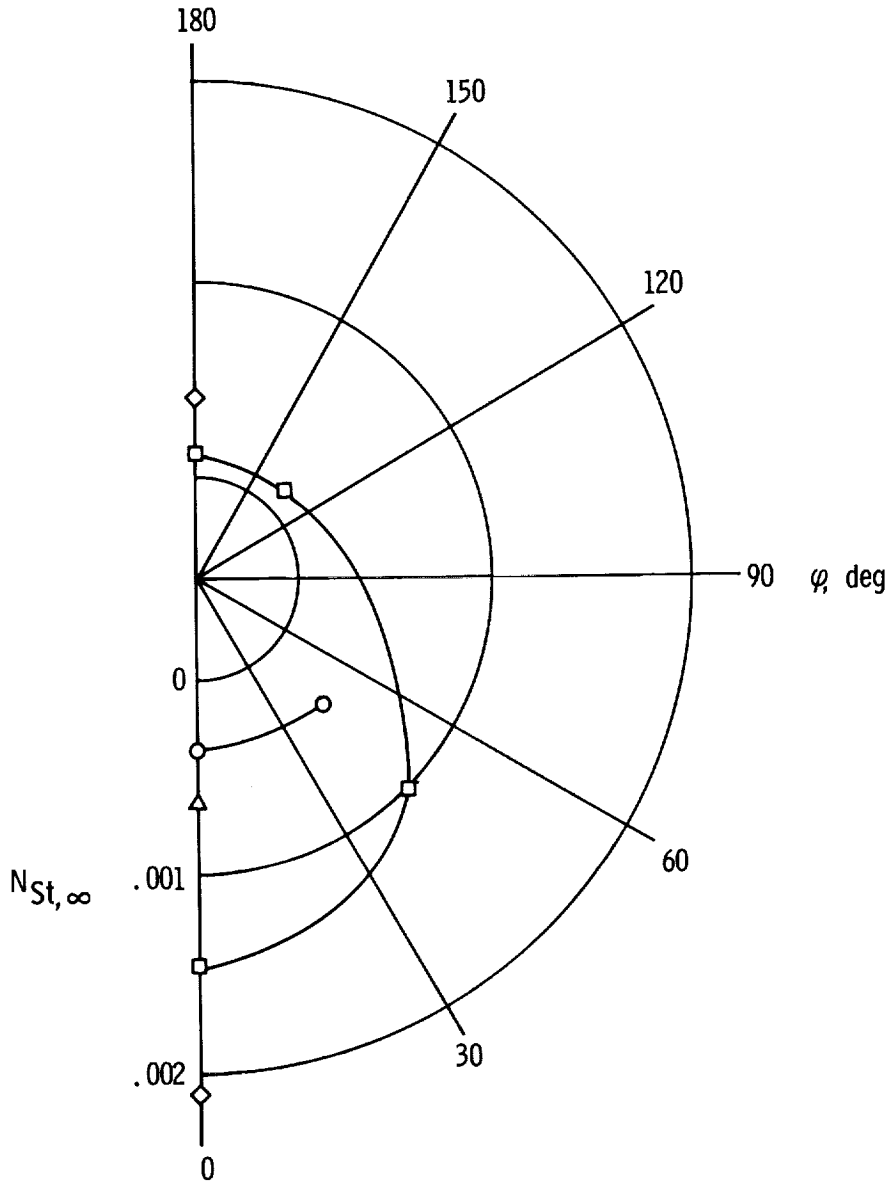

(e) $\frac{x_f}{l} = 0.309$.

Figure 7. – Continued.

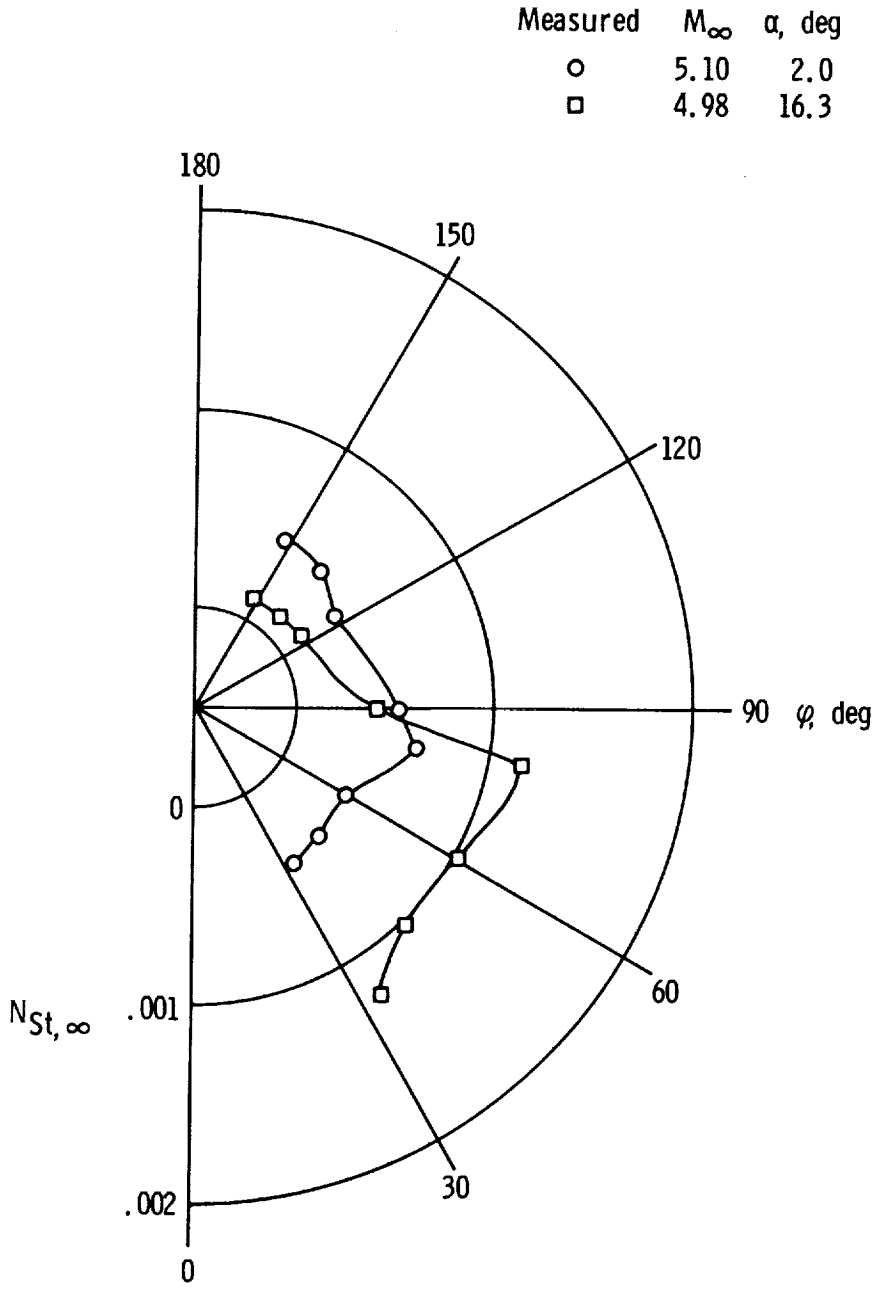

(f) $\frac{x_f}{l} = 0.343$.

Figure 7. – Continued.

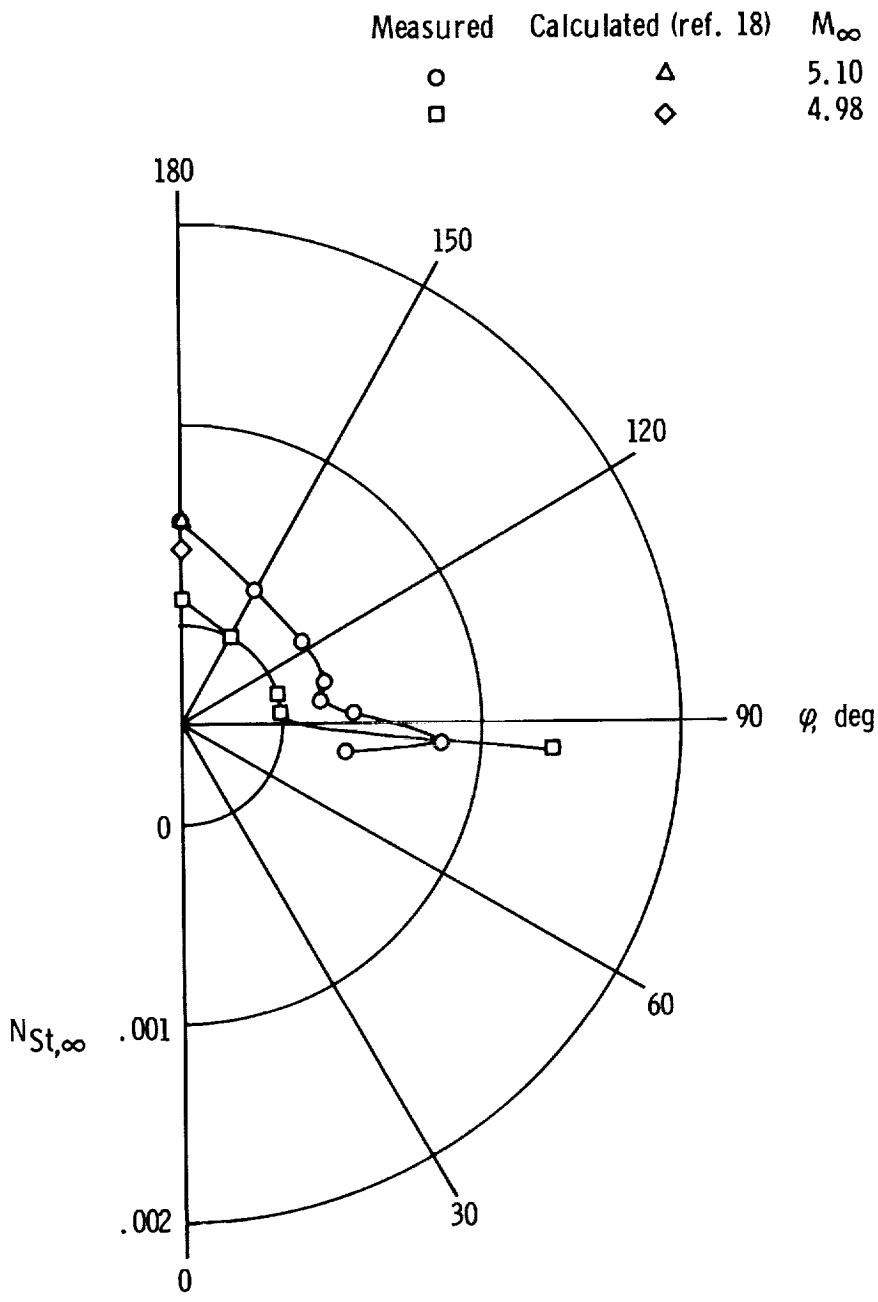

(g) $\frac{x_f}{l} = 0.567.$

Figure 7. – Concluded.

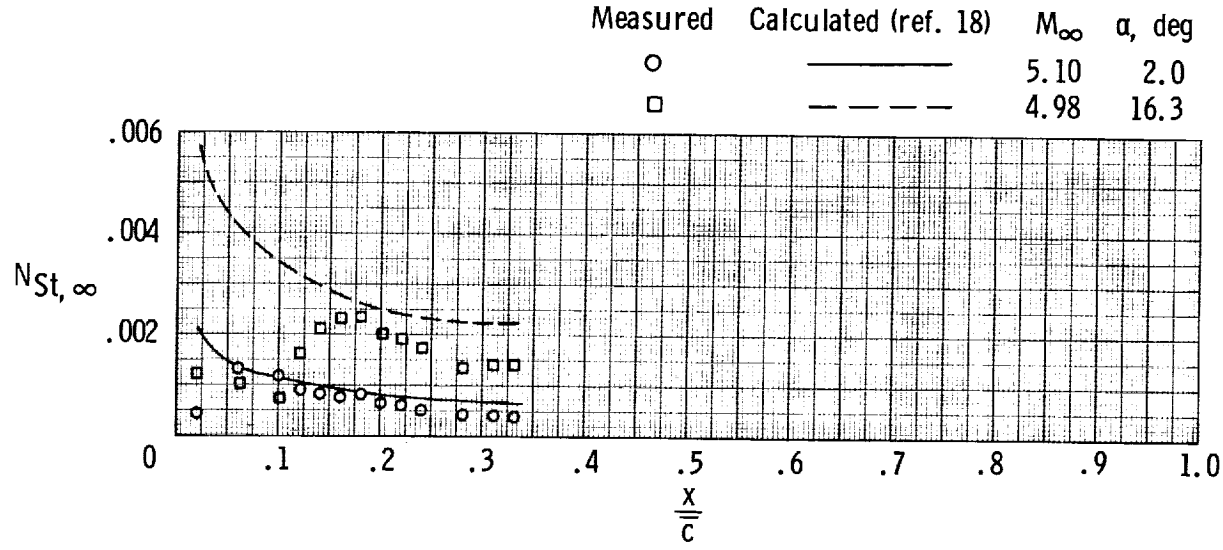

(a) $\frac{y}{b/2} = 0.953$.

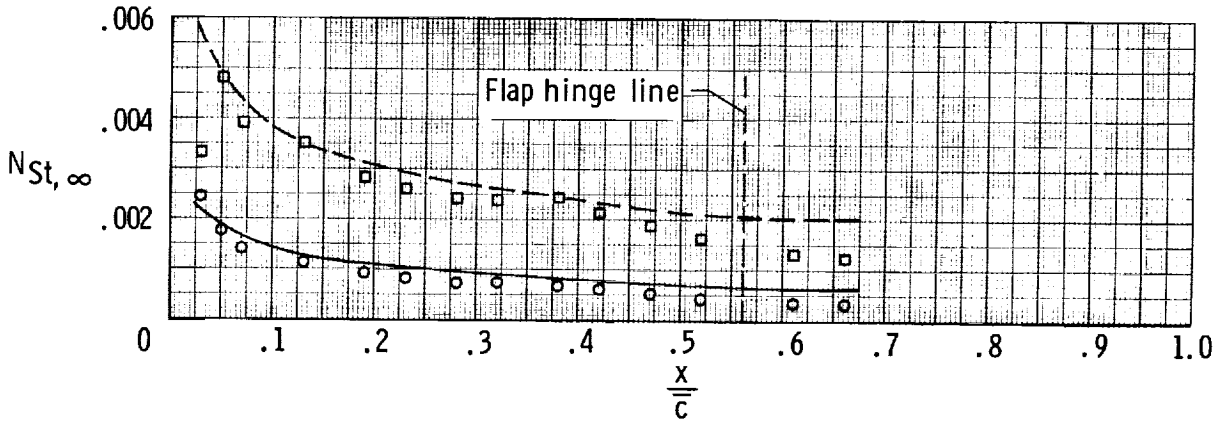

(b) $\frac{y}{b/2} = 0.629$.

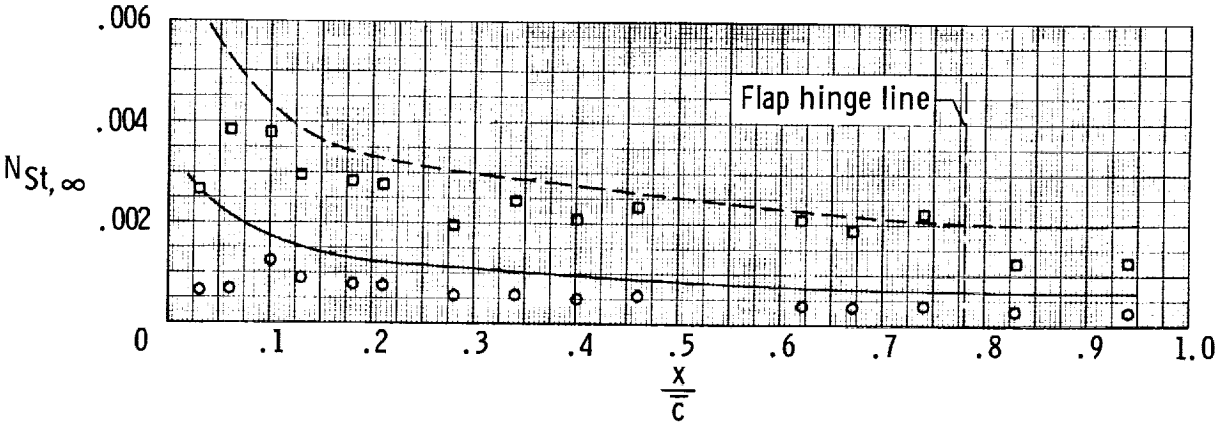

(c) $\frac{y}{b/2} = 0.357$.

Figure 8. – Effect of angle of attack on distribution of Stanton numbers on lower surface of wing.

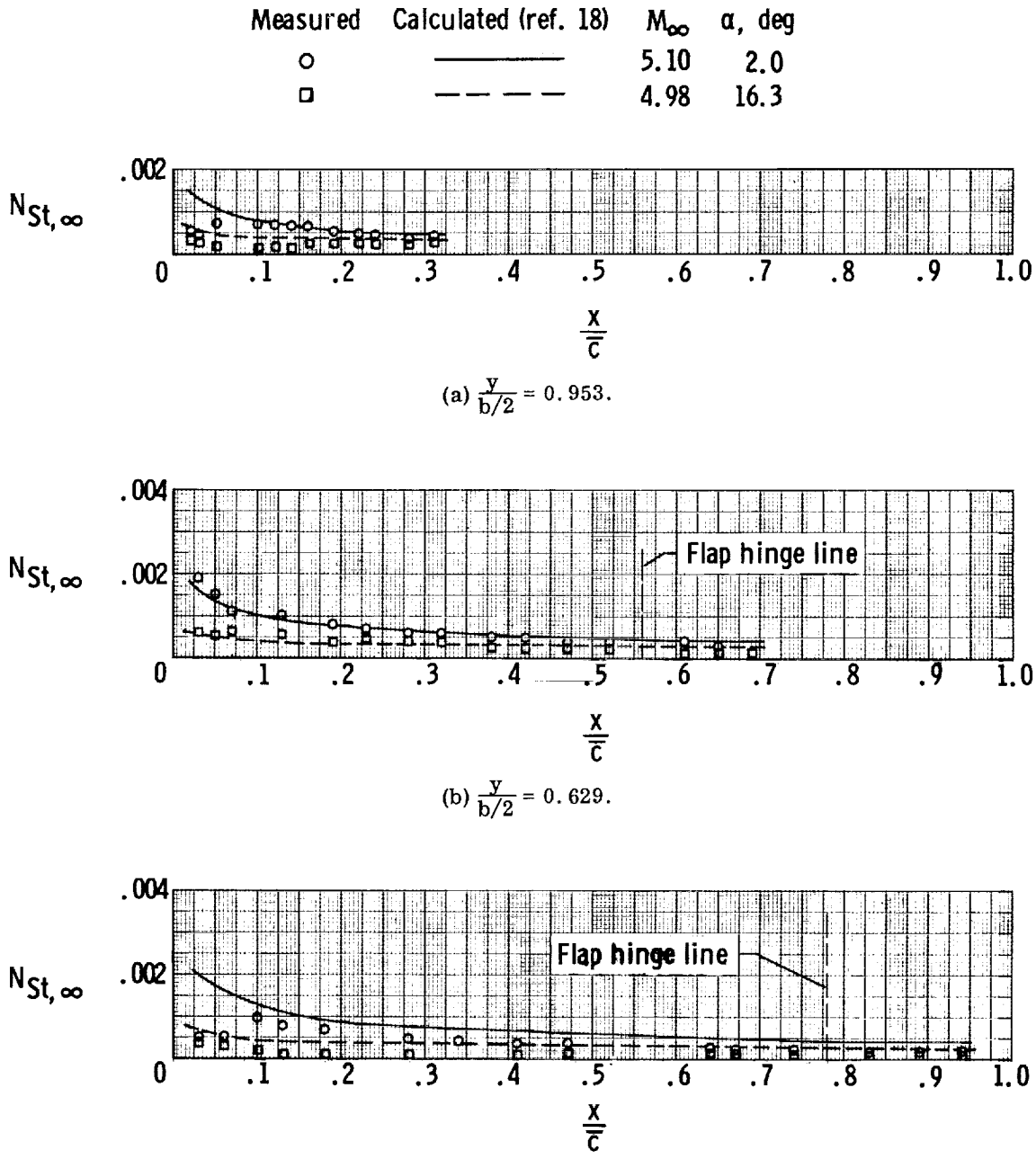

Figure 9.– Effect of angle of attack on distribution of Stanton numbers on upper surface of wing.

Measured	Calculated (ref. 18)	M_∞	α, deg
o	———	5.10	2.0
□	— — — —	4.98	16.3

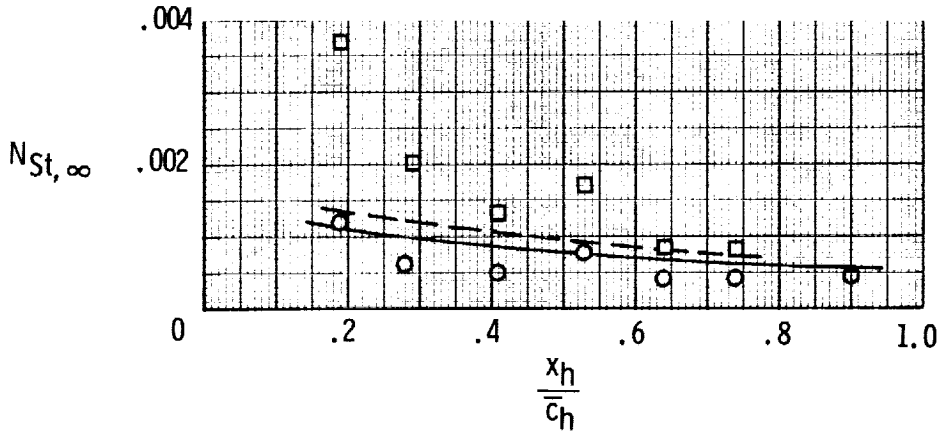

(a) Upper surface.

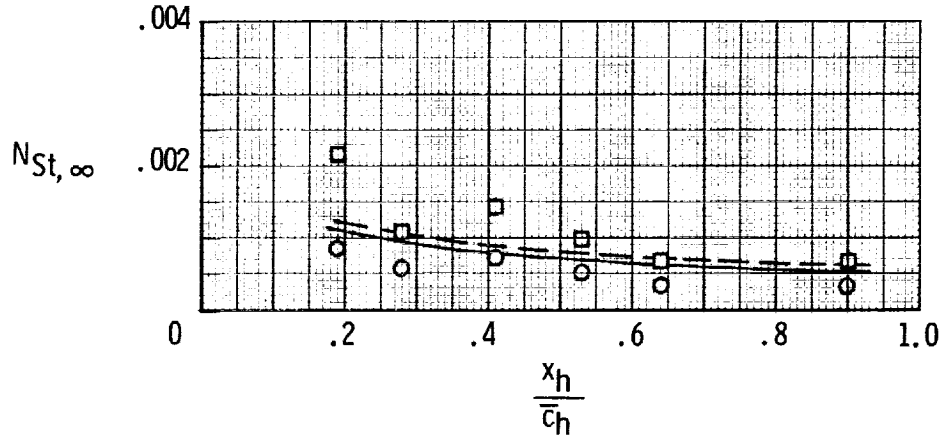

(b) Lower surface.

Figure 10. – Effect of angle of attack on distribution of Stanton numbers on horizontal tail.

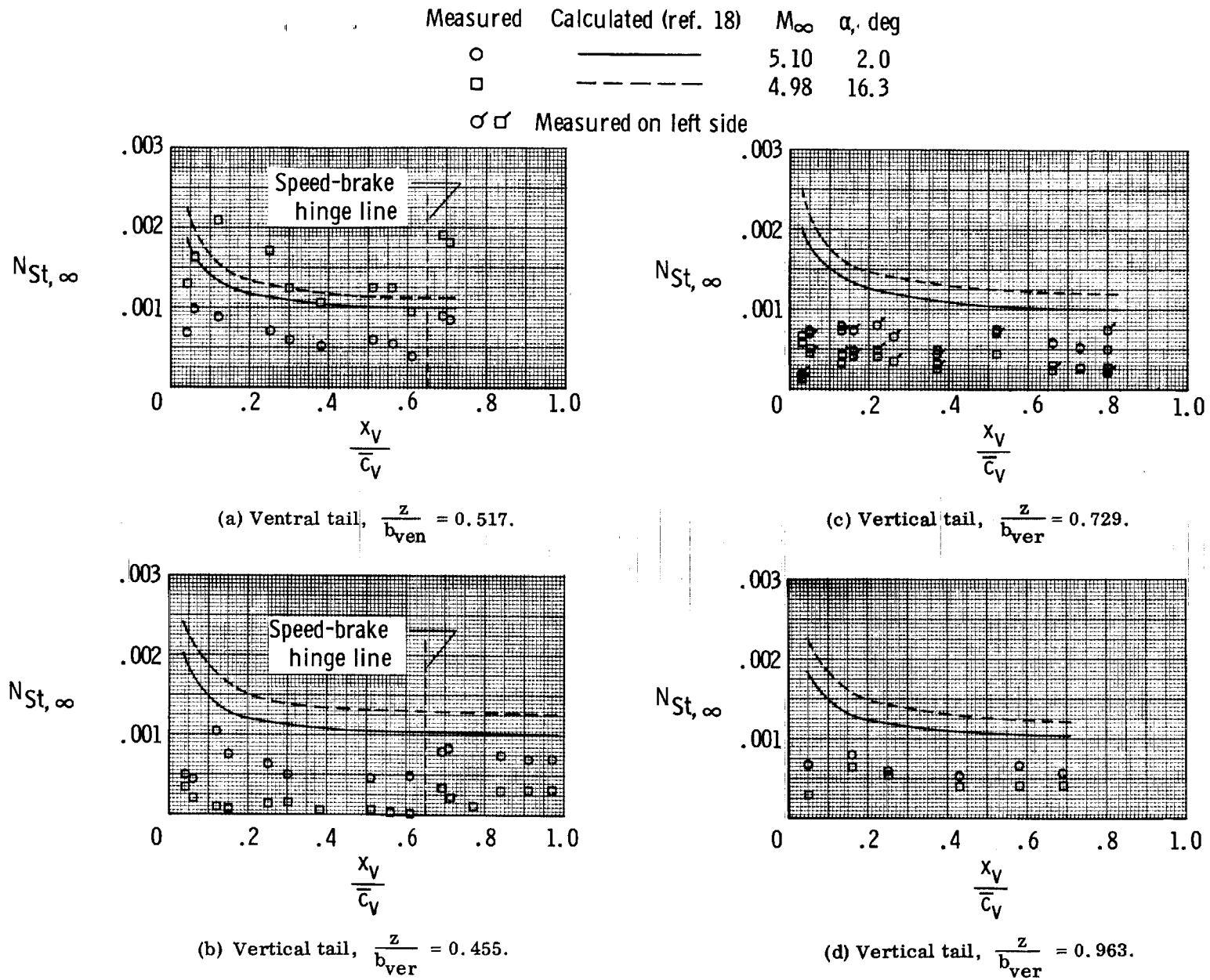

(a) Ventral tail, $\frac{z}{b_{ven}} = 0.517$.

(b) Vertical tail, $\frac{z}{b_{ver}} = 0.455$.

(c) Vertical tail, $\frac{z}{b_{ver}} = 0.729$.

(d) Vertical tail, $\frac{z}{b_{ver}} = 0.963$.

Figure 11.– Effect of angle of attack on distribution of Stanton numbers on ventral and vertical tails.

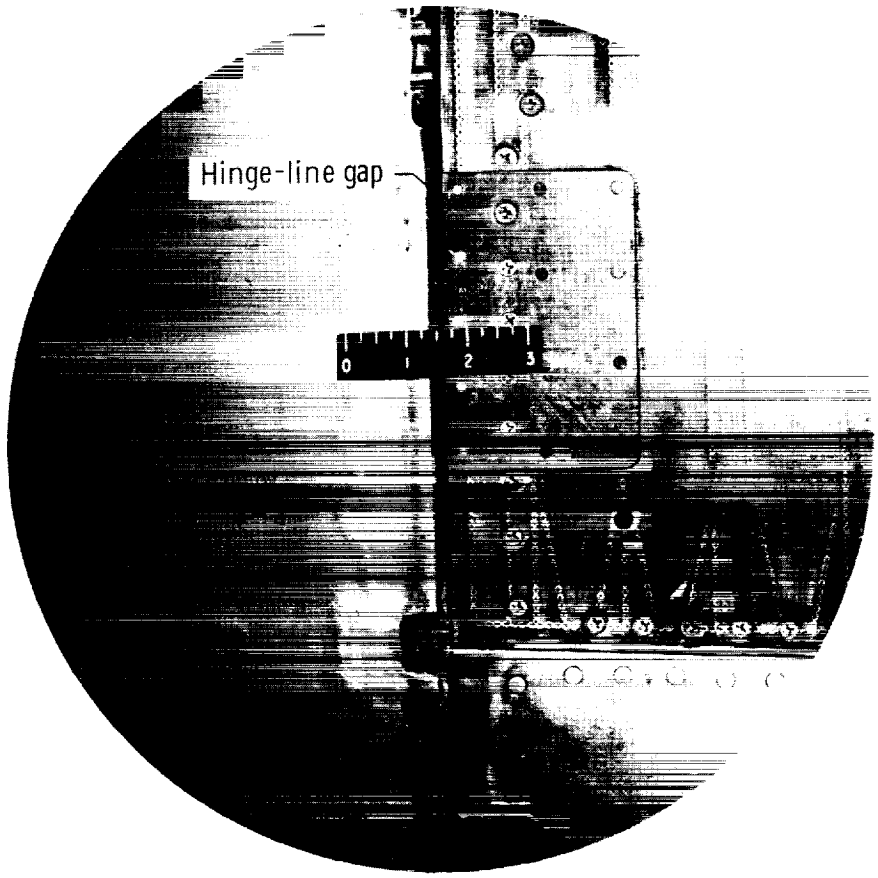

Detail A

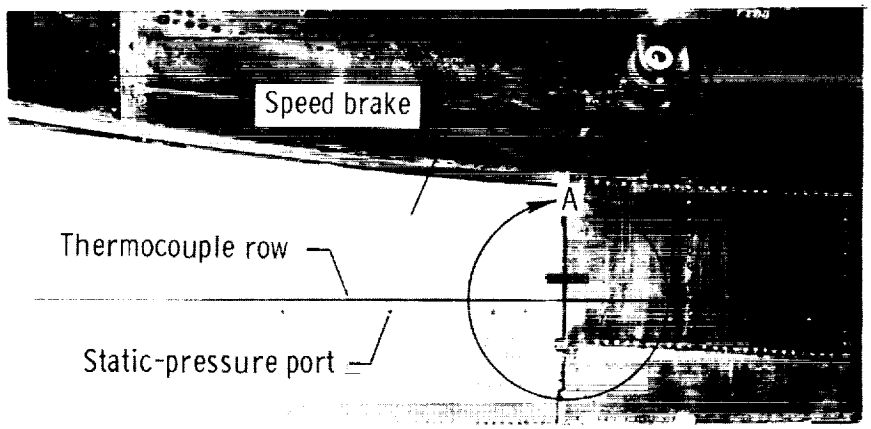

Figure 12. – Photograph of ventral tail showing discontinuity at speed-brake hinge area.

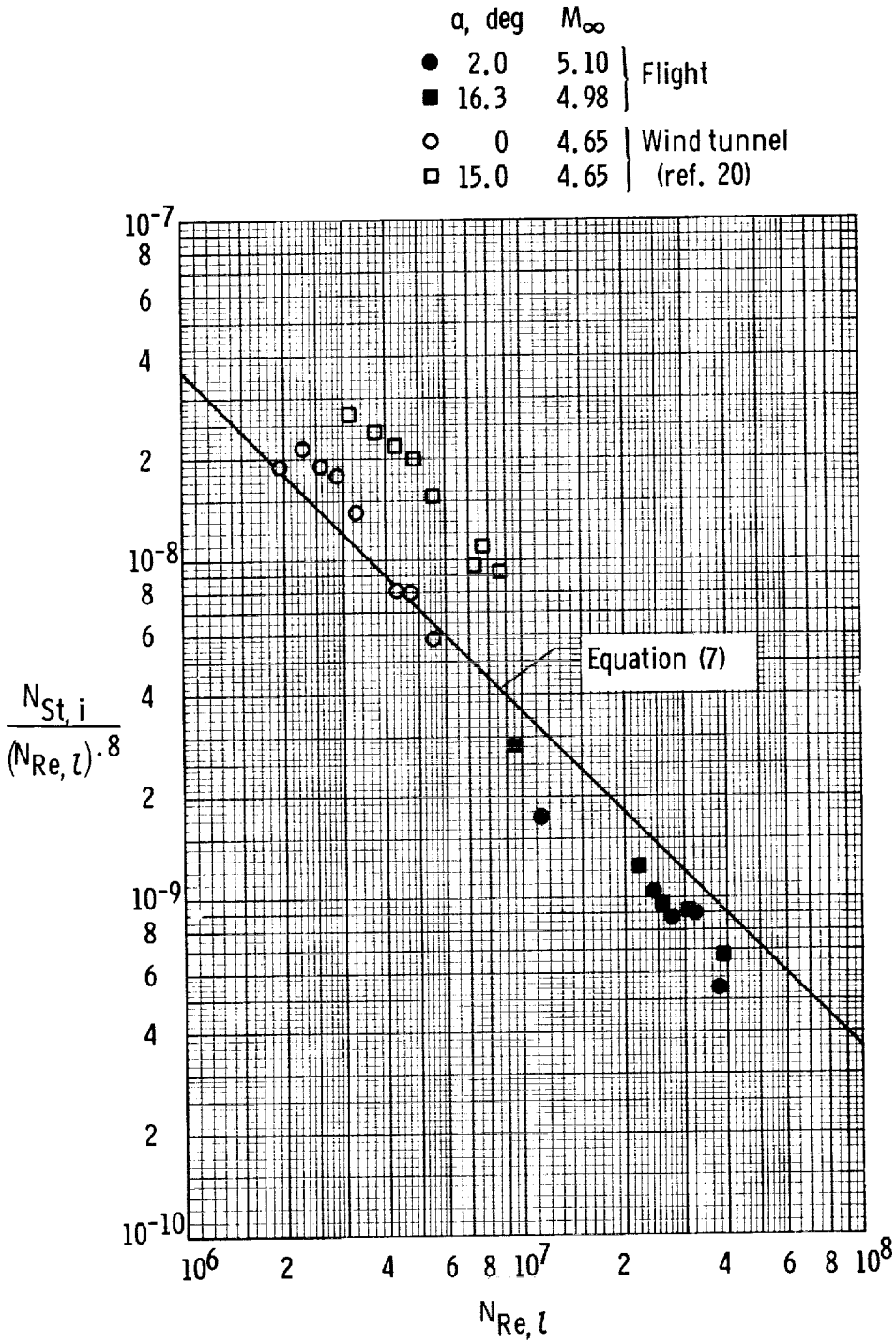

(a) Lower fuselage.

Figure 13. – Reynolds number correlation of wind-tunnel and flight data using Eckert's reference enthalpy method.

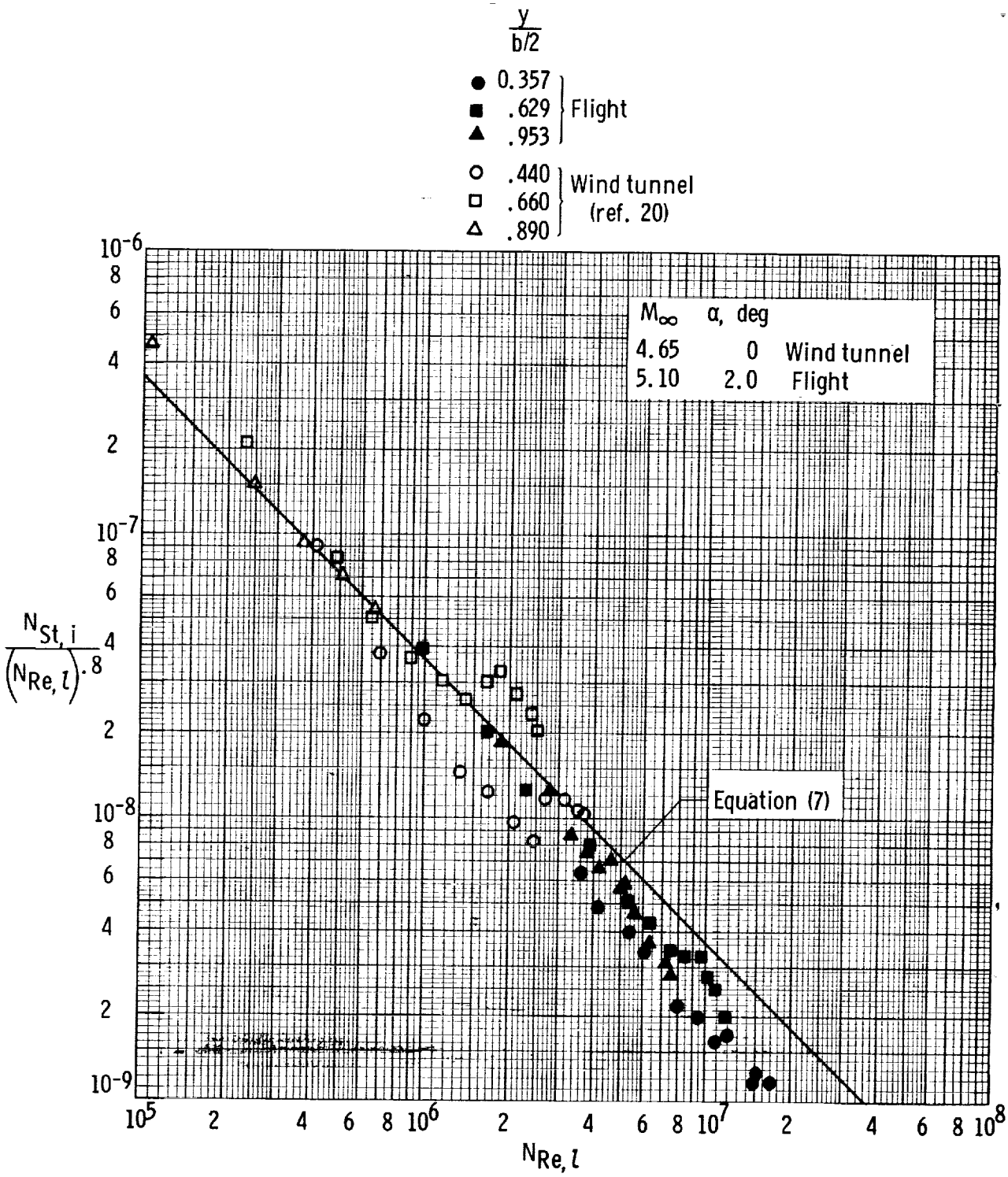

(b) Lower wing, low angle of attack.

Figure 13. – Continued.

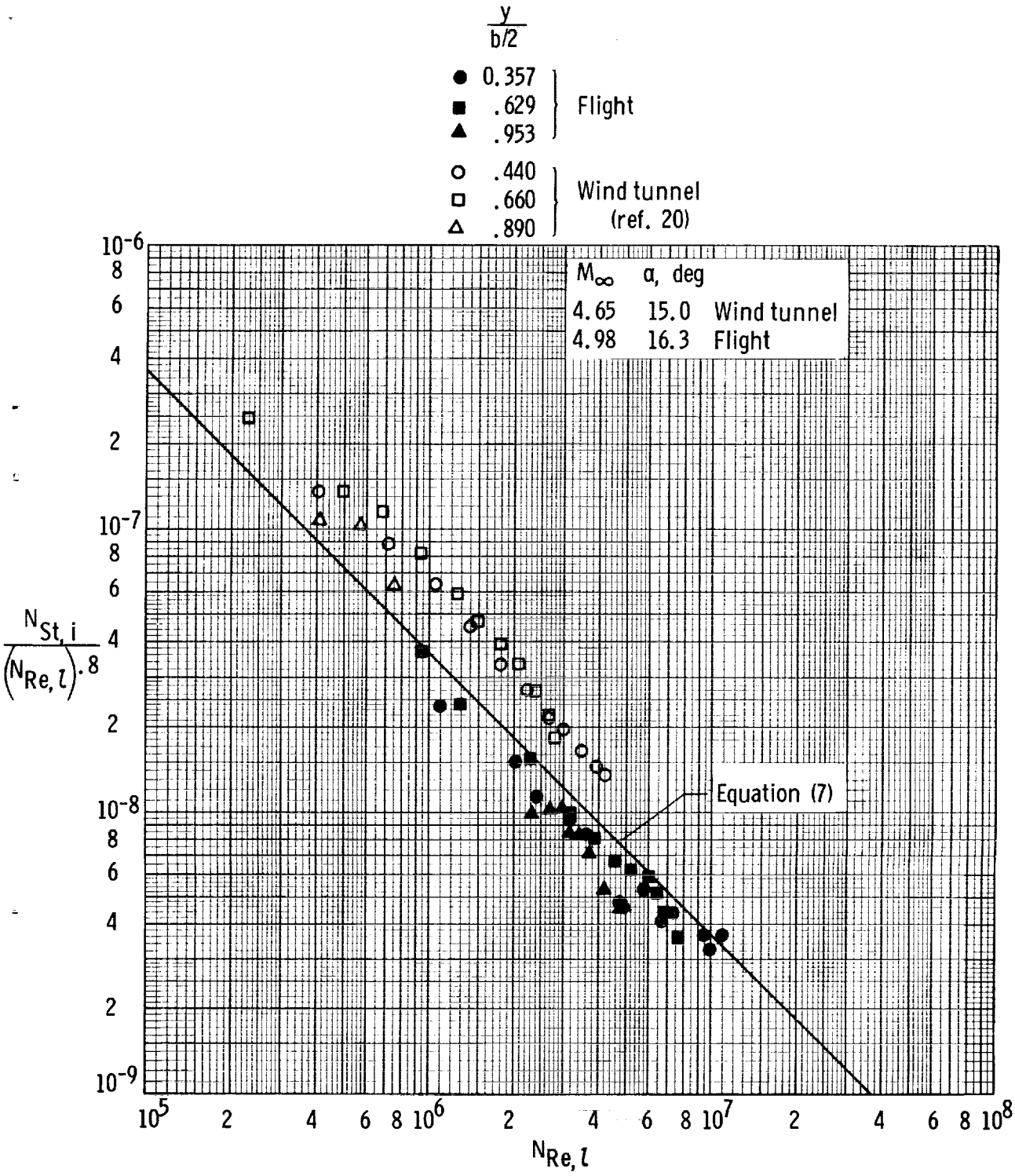

(c) Lower wing, high angle of attack.

Figure 13. – Continued.

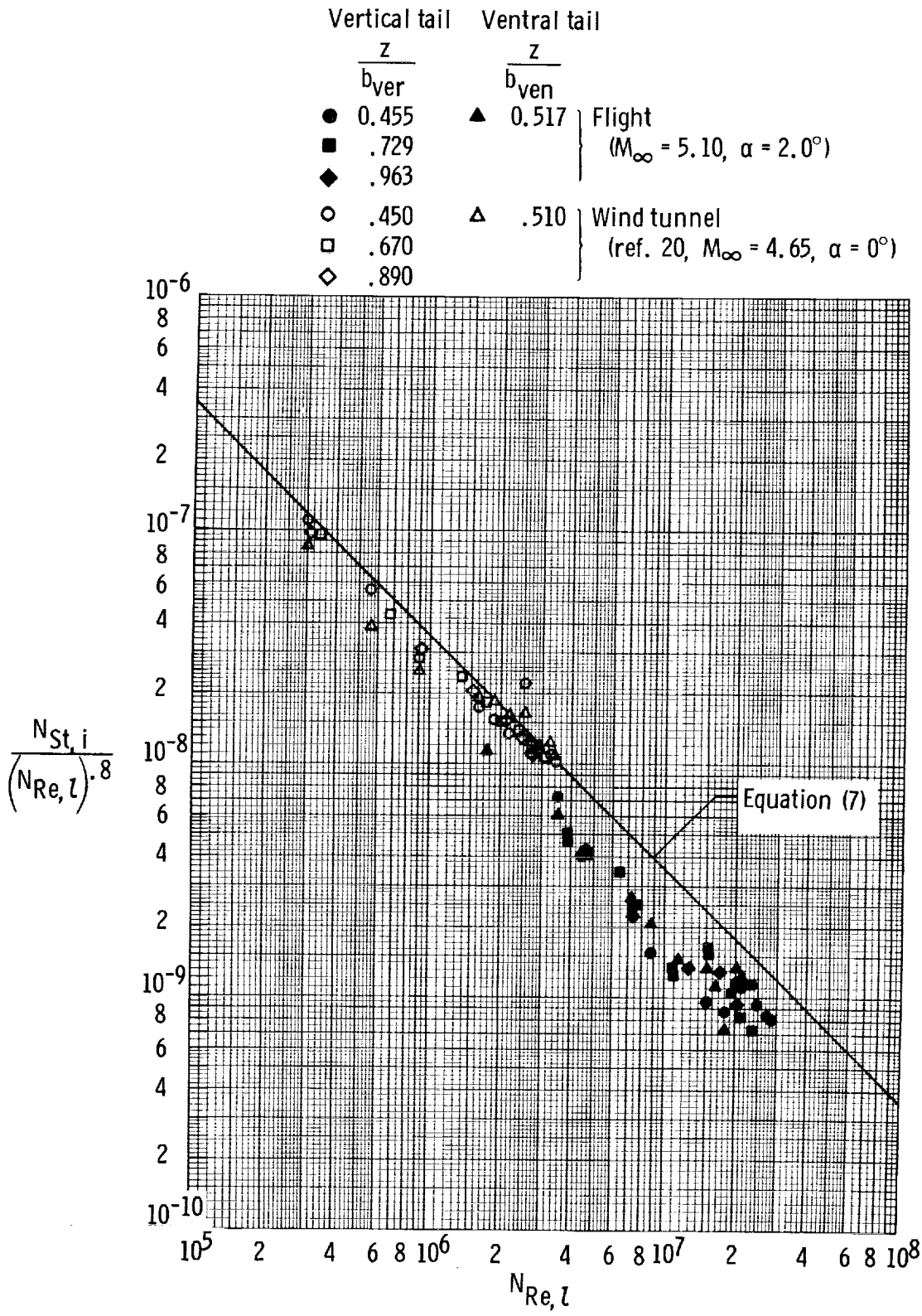

(d) Vertical and ventral tails, low angle of attack.

Figure 13. – Continued.

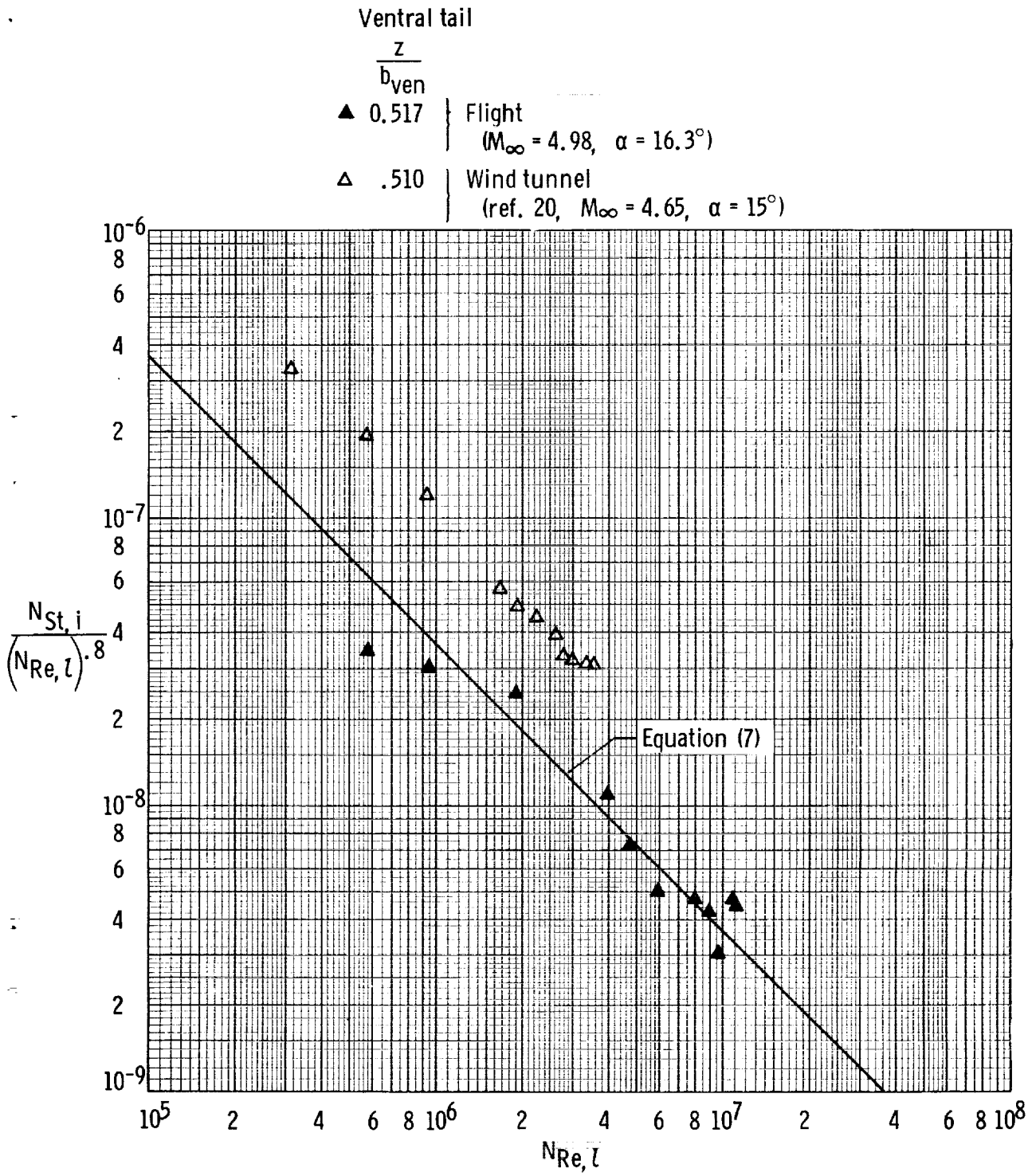

(e) Ventral tail, high angle of attack.

Figure 13. – Continued.

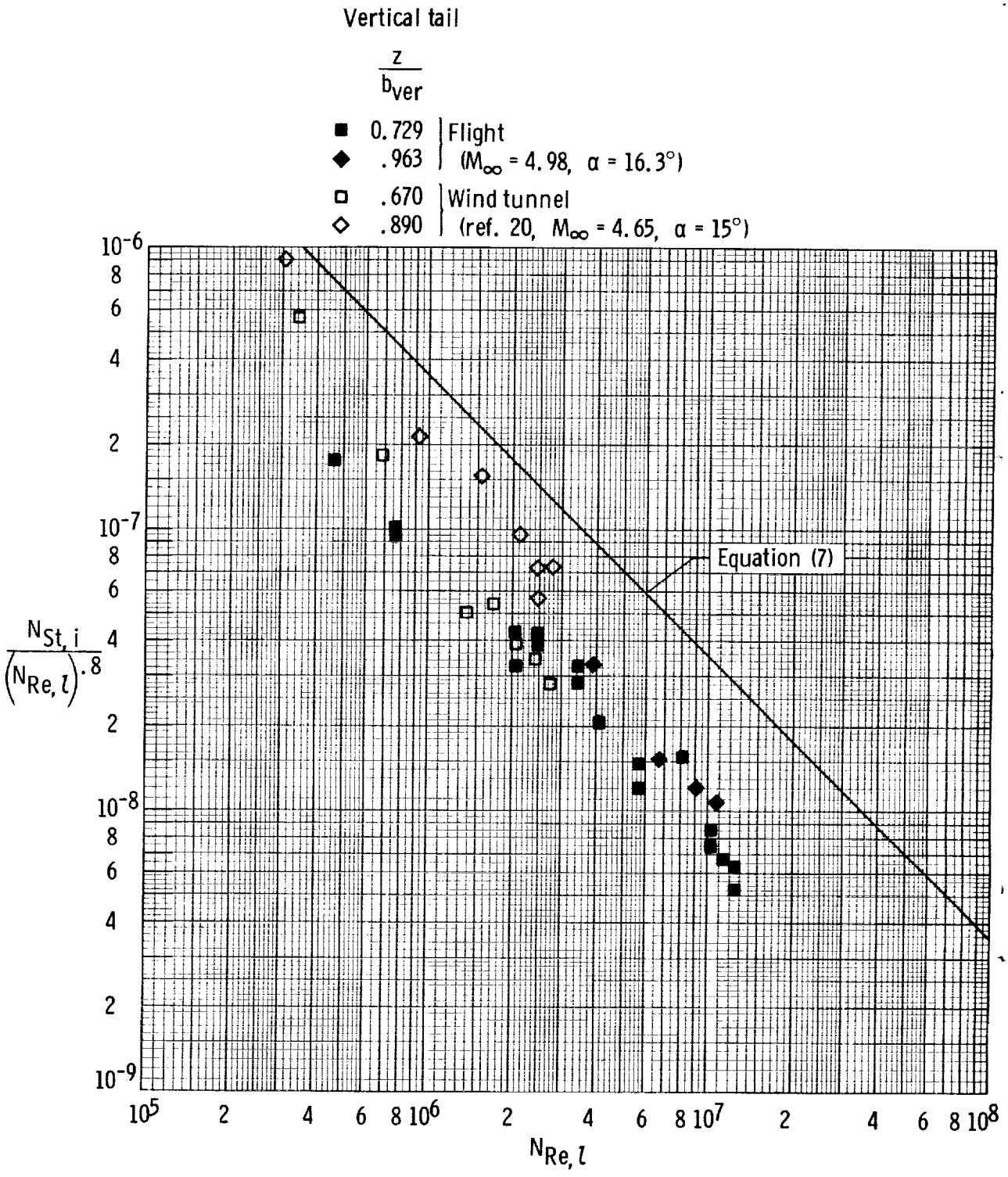

(f) Vertical tail, high angle of attack.

Figure 13. – Concluded.

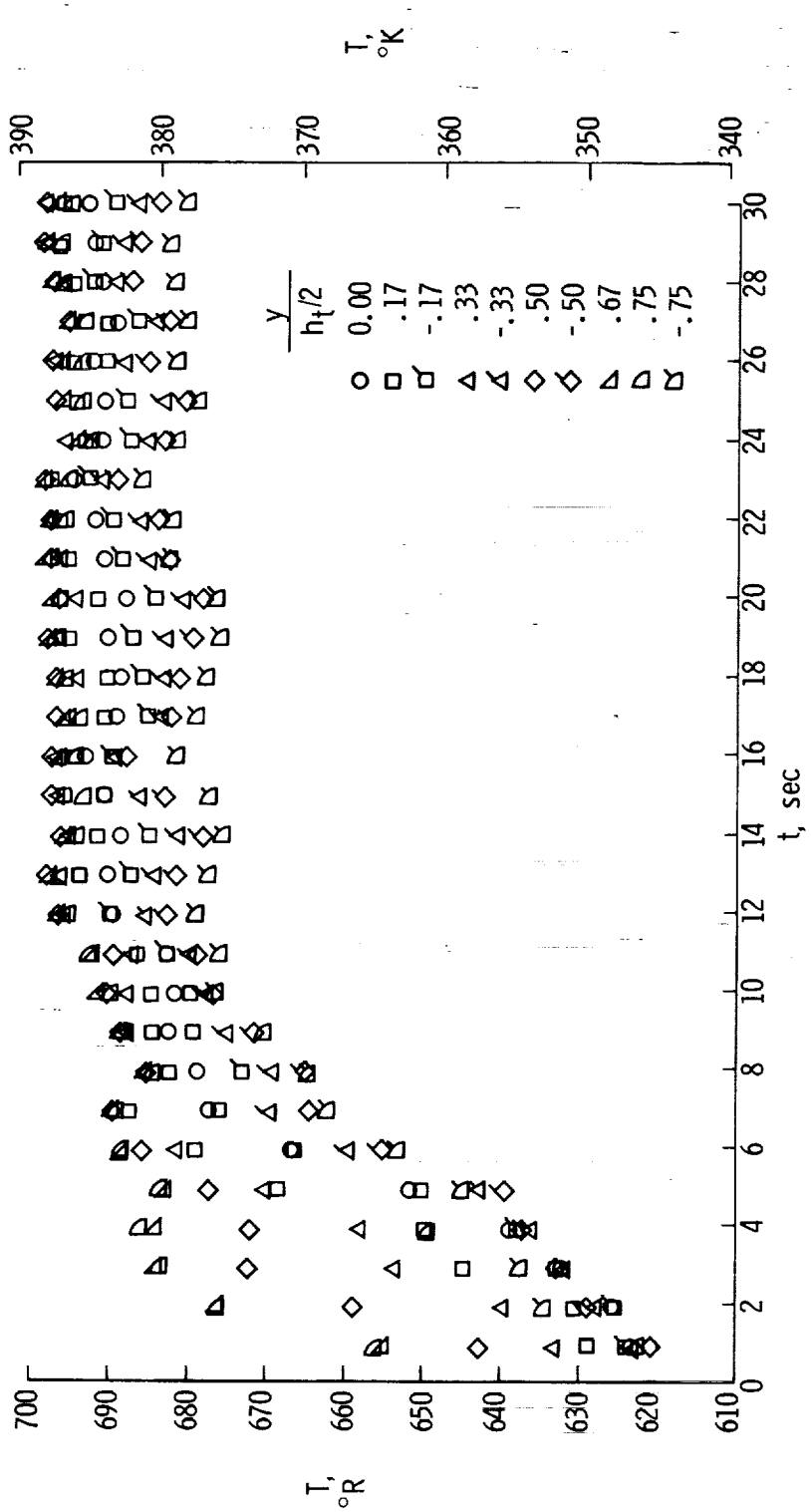

Figure 14. – Transient total-temperature distribution in the vertical plane of symmetry of the Langley Unitary Plan wind tunnel at $M = 4.65$, $\frac{h_t}{2} = 24$ in. (61 cm).

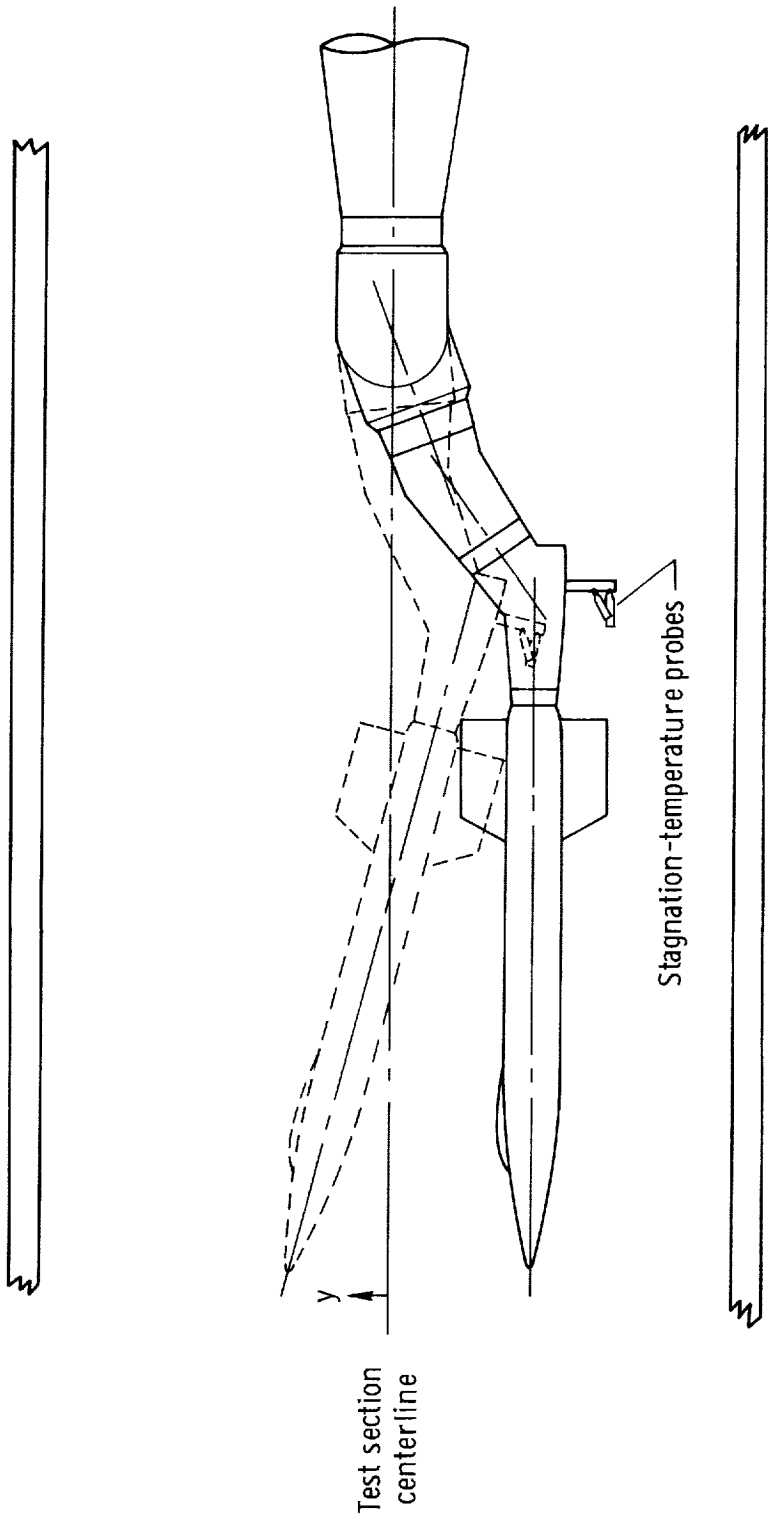

Figure 15. – Schematic side view of the 0.0667-scale model of the X-15 airplane in the Langley Unitary Plan wind tunnel.

"The aeronautical and space activities of the United States shall be conducted so as to contribute . . . to the expansion of human knowledge of phenomena in the atmosphere and space. The Administration shall provide for the widest practicable and appropriate dissemination of information concerning its activities and the results thereof."

NATIONAL AERONAUTICS AND SPACE ACT OF 1958

NASA SCIENTIFIC AND TECHNICAL PUBLICATIONS

TECHNICAL REPORTS: Scientific and technical information considered important, complete, and a lasting contribution to existing knowledge.

TECHNICAL NOTES: Information less broad in scope but nevertheless of importance as a contribution to existing knowledge.

TECHNICAL MEMORANDUMS: Information receiving limited distribution because of preliminary data, security classification, or other reasons.

CONTRACTOR REPORTS: Scientific and technical information generated under a NASA contract or grant and considered an important contribution to existing knowledge.

TECHNICAL TRANSLATIONS: Information published in a foreign language considered to merit NASA distribution in English.

SPECIAL PUBLICATIONS: Information derived from or of value to NASA activities. Publications include conference proceedings, monographs, data compilations, handbooks, sourcebooks, and special bibliographies.

TECHNOLOGY UTILIZATION PUBLICATIONS: Information on technology used by NASA that may be of particular interest in commercial and other non-aerospace applications. Publications include Tech Briefs, Technology Utilization Reports and Notes, and Technology Surveys.

Details on the availability of these publications may be obtained from:

SCIENTIFIC AND TECHNICAL INFORMATION DIVISION

NATIONAL AERONAUTICS AND SPACE ADMINISTRATION

Washington, D.C. 20546